Postharvest Biology and Technology 239 (2026) 114388

Contents lists available at ScienceDirect

Postharvest Biology and Technology

journal homepage: www.elsevier.com/locate/postharvbio

Modulated UV-C radiation as an innovative strategy for postharvest disease control and quality preservation in papaya and orange fruits

Adriane Maria da Silva [a,*], Daniel Terao [b], Itala Suzana Oliveira Silva [c], Aline de Holanda Nunes Maia [b], Washington Luiz de Barros Melo [d], Katia de Lima Nechet [b], Bernardo de Almeida Halfeld-Vieira [b], Elke Simoni Dias Vilela [b], Juliana Aparecida Fracarolli [a]

[a] Universidade Estadual de Campinas (UNICAMP), School of Agricultural Engineering (FEAGRI), Postharvest Technology Laboratory, Cidade Universitária Zeferino Vaz, Barão Geraldo, Campinas, SP 13083-970, Brazil
[b] Embrapa Meio Ambiente, Empresa Brasileira de Pesquisa Agropecuária, Jaguariúna, SP CP 69-13918-110, Brazil
[c] Universidade Federal da Bahia (UFBA), Postgraduate Program in Food Science, Salvador, BA 40170-110, Brazil
[d] Embrapa Instrumentação Agropecuária, Empresa Brasileira de Pesquisa Agropecuária, São Carlos, SP 13561-206, Brazil

ARTICLE INFO

Keywords:
Papaya
Orange
Photothermal effect
Alternative control
Resistance induction

ABSTRACT

Postharvest losses remain a major challenge in fruit production systems, affecting both climacteric fruits, such as papaya, and non-climacteric fruits, such as orange. Ultraviolet-C (UV-C) radiation has emerged as a sustainable alternative to chemical fungicides; however, its effectiveness depends on the applied dose and radiation delivery mode. This study investigated the comparative effects of continuous and frequency-modulated UV-C radiation on postharvest disease control and fruit quality on papaya and orange. Two independent experiments were conducted. Experiment 1 evaluated the influence of modulation frequencies (0, 15, 30, and 45 Hz) on disease progression, while Experiment 2 combined the most effective frequencies with different exposure times to define optimal treatment conditions. In papaya, UV-C modulation at 30 Hz/20 s (0.44 kJ m^{-2}) provided effective control of anthracnose (67% reduction in incidence), while minimizing photothermal damage, with no visible epidermal injuries. In orange, continuous UV-C radiation (0 Hz) applied for 30 s (1.99 kJ m^{-2}), completely suppressed sour rot development (100%) without visible peel injury. Therefore, the selection of the UV-C radiation application mode is species-specific. Notably, modulation of UV-C irradiation has demonstrated enhanced efficiency in postharvest disease control while reducing epidermal burn. Additionally, the treatments stimulated defense responses, as evidenced by increased activities of phenylalanine ammonia-lyase, polyphenoloxidase, peroxidase, and catalase. Physicochemical analyses confirmed the maintenance of firmness, acidity, and color stability, indicating the preservation of postharvest quality in both fruits. Overall, modulated UV-C radiation represents a promising non-chemical postharvest technology, enabling efficient disease control while maintaining fruit quality.

1. Introduction

Postharvest losses of fruits represent a significant challenge for the production chain, particularly during storage and transport (Rajapakshe et al., 2025), and can range from 20% to 40% of the harvested volume, depending on fruit species and management conditions (Seshadri et al., 2024). Papaya of the 'Papaia' variety (*Carica papaya* L.) and orange of the 'Lima' variety (*Citrus sinensis* L.) are examples of economically important fruits whose distinct physiological characteristics directly influence their shelf life and susceptibility to postharvest losses (Bornal et al., 2021).

Papaya is a climacteric fruit characterized by rapid postharvest ripening, high respiratory activity, and ethylene production, making it highly perishable and susceptible to diseases such as anthracnose (*Colletotrichum gloeosporioides*). Its thin and delicate peel further increases vulnerability to pathogen attack (Kabir and Hossain, 2025). In contrast, orange is a non-climacteric fruit with a more stable postharvest metabolism and a relatively thick peel that provides greater physical protection; however, it remains susceptible to pathogens such as *Geotrichum citri-aurantii* (Khamsaw et al., 2022), the causal agent of sour rot disease.

* Corresponding author.
E-mail address: adriane.silva@feagri.unicamp.br (A.M. Silva).

https://doi.org/10.1016/j.postharvbio.2026.114388
Received 20 January 2026; Received in revised form 15 April 2026; Accepted 17 April 2026
Available online 20 April 2026

Traditional postharvest disease management relies on chemical fungicides such as thiabendazole and imazalil, but their continuous use raises concerns regarding toxicity, chemical residues, and the development of fungal resistance (Islam et al., 2024; Sasaki et al., 2024). Sustainable alternatives such as ultraviolet-C (UV-C) radiation have gained prominence due to their germicidal effect, which induces thymine dimers in microbial DNA and triggers defense responses in plant tissues without leaving chemical residues (Gąstoł and Błaszczyk, 2024; Terao et al., 2021). Its efficacy depends on the fruit species, the dose, the mode of application, and the microorganism's sensitivity (Mansur et al., 2023).

UV-C radiant energy can be applied in different emission modes. Most postharvest studies have evaluated continuous irradiation (Phannakham et al., 2026; Rutigliano et al., 2025), in which emission is uninterrupted, remaining constant and uniform throughout the treatment period without variations in intensity. Intermittent modes such as pulsed UV-C have also been investigated (Cui et al., 2026; Wang et al., 2025); in these systems, radiation is delivered as extremely short, high-intensity flashes lasting microseconds or milliseconds (Scolfaro et al., 2007; Söbeli et al., 2021), which differ from modulated exposure in terms of energy distribution (Scolfaro et al., 2007).

In contrast, modulated UV-C radiation, still little explored in postharvest research, alternates illuminated and dark periods in controlled cycles while maintaining constant intensity during each illuminated phase, typically generated by mechanical choppers (Scolfaro et al., 2007). This produces a square-wave emission pattern in which the total dose may be maintained constant while the temporal distribution of energy changes, potentially influencing microbial inactivation, fruit physiological responses, and photothermal effects - localized heating caused by UV-C absorption (Scolfaro et al., 2007). Such modulation may allow treatments to be tailored to different fruit species based on epidermal sensitivity, reducing surface heating while maintaining treatment effectiveness. As most published studies focus on continuous irradiation and only a limited number evaluate alternative emission regimes, the effects of modulated UV-C on postharvest disease control and fruit quality remain poorly understood.

In addition to possible effects on pathogens, UV-C radiation may stimulate biochemical defense mechanisms in fruit tissues. Activities of enzymes such as peroxidase, polyphenol oxidase, phenylalanine ammonia-lyase, and catalase are commonly measured as indicators of induced resistance in postharvest studies (Dixon, 2001; Maldonado et al., 2015).

Thus, the present study aimed to evaluate the effect of UV-C radiation applied in continuous and modulated modes on disease control and postharvest quality of two fruit species, papaya (climacteric) and orange (non-climacteric).

2. Materials and methods

2.1. Fungal isolates from orange and papaya

The fungal isolates of *G. citri-aurantii* (CMAA 1841, from orange) causal agent of the sour rot disease and from *C. gloeosporioides* (CMAA 1490, from papaya), the causal agent of anthracnose, were obtained from the Collection of Microorganisms of Agricultural and Environmental Importance (CMAA, AleloMicro Consultas, 2025) of Embrapa Meio Ambiente, Jaguariúna, São Paulo, Brazil.

2.2. Fruits preparation and inoculation

Papaya fruit var. 'Papaia' at ripening stage 2 - characterized by green peel with up to 25% yellowing on the surface (Programa Brasileiro para Modernização da Horticultura, 2003) - were purchased at the CEASA - Centrais de Abastecimento in Campinas, São Paulo, Brazil.

Orange fruit var. 'Lima' at stage 3, corresponding to a fully orange-colored peel (Programa Brasileiro para Modernização da Horticultura, 2011), was obtained from local growers in the same region. None of the fruit had received any prior postharvest fungicide treatment.

The fruit were washed with water and neutral detergent, rinsed, and dried with paper towels. They were then wounded at the equatorial region using a stainless-steel needle (1 mm diameter × 3 mm depth) and inoculated with 10 μL of a spore suspension adjusted using a Neubauer chamber. Orange fruit were inoculated with *G. citri-aurantii* at 10^6 spores mL^{-1} , and papaya fruit were inoculated with *C. gloeosporioides* at 10^6 spores mL^{-1} .

After inoculation, orange fruit were placed in plastic boxes with lids and maintained in a humid chamber for 4 h at 22 ± 2 °C in the dark (Da Silva et al., 2023), whereas papaya fruit remained under the same conditions for 24 h (Ribeiro et al., 2016). The sealed boxes generated a near-saturated humidity environment (95 ± 2% RH), which is commonly used in postharvest inoculation experiments to promote pathogen infection. Control fruit (without treatment) was maintained under identical temperature, humidity, and lighting conditions as the treated fruit. The different incubation periods were selected according to the infection characteristics of each host–pathogen system.

After the incubation period, the inoculated papaya and orange fruits were subjected to continuous and modulated UV-C treatments. Immediately after UV-C exposure, the fruits were stored for 30 min in the dark to prevent photoreactivation (Duque-Sarango et al., 2023).

2.3. UV-C radiation treatment

UV-C radiation was applied using a prototype developed by Embrapa Instrumentação, operating in continuous and modulated modes. The device includes an internal cylindrical mirror that reflects and collimates the radiation, ensuring uniform illumination of the fruit surface. The system uses three longitudinally arranged UV-C fluorescent lamps (Philips, TUV 36T5HE, 254 nm) that can be activated individually depending on the fruit's sensitivity (Figure S1). Before the experiments, preliminary sensitivity tests were conducted to define the number of UV-C lamps for each fruit. Papaya and orange fruits were exposed to different lamp configurations, and papaya showed visible injury under three lamps, whereas the orange tolerated this condition. Therefore, two lamps were used for papaya and three lamps (all activated) for orange in all subsequent experiments (preliminary *in vitro* test, *in vivo* experiments, quality and enzymatic analysis).

Fruits were positioned on a coaxial cylindrical metal grid to ensure homogeneous radiation exposure. Before treatment, the lamps were turned on for 20 min to stabilize emission. Light modulation was achieved using a cylindrical mechanical chopper with three symmetrical longitudinal openings, continuously rotating and driven by an alternating-current electric motor controlled by an electronic circuit that also governs lamp operation. As the chopper rotates, the openings intermittently allow radiation to pass, producing a square-wave beam (Figure S2).

2.4. Calculation of radiation dose

The sequence of calculations required for determining the total dose for both UV-C application modes, modulated or continuous, expressed as the energy applied corresponding to each treatment, is described below. Detailed definitions of the terms used in the equations are provided in the Supplementary Material (Table S1, Bolton, (2000)).

The modulation frequency (f_{ch}) was determined by the product of the number of chopper openings (n, in this study n = 3) and the chopper rotation speed (Speed, in revolutions per minute, RPM), considering 60 as the conversion factor to express frequency in Hertz (Hz):

$$f_{ch} = \frac{n \bullet Speed}{60} \text{ and, with } n = 3: \quad f_{ch} = \frac{Speed}{20} \tag{1}$$

During half of the modulation period (T/2), the fruit receives radiation, while during the other half, it remains in the dark. The energy

emitted in each semi-period ($E_{T/2}$, J m^{-2}) is obtained by dividing the light irradiance (E, W m^{-2}) by two and adjusting for the modulation frequency (f_{ch}, Hz):

$$E_{T/2} = \frac{1}{2}\frac{E}{f_{ch}} \quad (2)$$

The number of radiation pulses received by the fruit in each semi-period ($N_{T/2}$) during the time the lamps remained on (t_{on}, seconds) is determined by multiplying the exposure time by the modulation frequency (f_{ch}, Hz):

$$N_{T/2} = t_{on} \bullet f_{ch} \quad (3)$$

The total accumulated energy (E_T, J m^{-2}), corresponding to the product of the energies delivered in each semi-period ($E_{T/2}$, J m^{-2}) and the respective number of pulses ($N_{T/2}$), is calculated as:

$$E_T = N_{T/2} \bullet E_{T/2} \quad (4)$$

For continuous (non-modulated) radiation, there is no interruption of the light beam; therefore, all energy emitted during the exposure time (t_{on}, seconds) is absorbed by the fruit. The total accumulated UV-C energy (E_T, J m^{-2}) is calculated as a function of the exposure time (t_{on}) and the irradiance (E, W m^{-2}):

$$E_T = t_{on} \cdot E \quad (5)$$

To express the total accumulated energy (E_T) in kJ m^{-2}, the value is divided by 1000.

The irradiance incident on the fruit surface is determined using a digital radiometer (Genuv – MG-07.1 GUVX-T1XGS7.1-LA9) equipped with a UV-C sensor. The sensor is positioned on the same plane and at the same distance as the fruit exposed to the lamps, ensuring equivalent experimental conditions. Readings are recorded once the light output stabilizes, and the mean irradiance (W m^{-2}) is recorded.

The direct irradiance (E) on the fruit surface at a distance of 25 cm from the lamps is estimated at 22.1 W m^{-2} per lamp (Philips Lighting, 2022). Because the UV-C radiation emitted by the lamps strikes the fruit surface predominantly in a collimated manner, the fluence rate (E′) and irradiance (E) are considered equivalent (Bolton, 2000).

2.5. Experiments to evaluate the effect of UV-C radiation on disease progression in papaya and orange fruits

2.5.1. Photothermal monitoring

To estimate the photothermal behavior of the irradiation system, the temperature inside the equipment chamber during UV-C exposure was monitored prior to the experiments using a digital thermometer (Unity THU-200 thermohygrometer) coupled to a thermocouple. The thermocouple was positioned inside the chamber, on a section of rigid expanded polystyrene (EPS) board, a thermal insulation, which served as a physical support for the thermocouple. This setup allowed comparison of the photothermal effects of continuous and modulated UV-C radiation on a standardized surface. Temperature readings were recorded at 1 min intervals.

2.5.2. In vivo experiments with papaya and orange fruits

Four *in vivo* experiments were conducted: two designed to compare continuous and modulated UV-C radiation under a fixed exposure time (P1 with papaya fruit and O1 with orange fruit), and two additional experiments evaluating combinations of modulation frequency and exposure time (P2 with papaya fruit and O2 with orange fruit). The Supplementary Material includes a schematic workflow of the *in vivo* experiments (Figure S3).

2.5.2.1. Experiment 1 (P1 and O1): effect of continuous and modulated UV-C radiation under fixed exposure time. In experiments P1 (papaya) and O1 (orange), five treatments were evaluated: a non-irradiated control and four UV-C treatments with a fixed exposure time (t_{on} = 30 s) and modulation frequencies (f_{ch}) of 0 (continuous), 15, 30, or 45 Hz (Table 1). The experimental design was a completely randomized design (CRD) with 10 replicates (fruit) per treatment for papaya and 8 replicates per treatment for orange (Table 1). Each experiment (P1 and O1) was performed twice, using different batches of fruit under the same experimental conditions.

The exposure time of 30 s was selected based on a preliminary *in vitro* test (Figure S4), in which this duration resulted in the greatest reduction in colony-forming units and was therefore adopted for the first *in vivo* experiment. The preliminary test was conducted using a CRD, with four replicates (plates) per treatment, and exposure times of 0 (control), 15, 30, 45, and 60 s under continuous UV-C irradiation (0 Hz). Colony-forming units were quantified after incubation at 22 ± 2°C and 70 ± 2% relative humidity for 3 days, and the results were analyzed using polynomial regression (Figure S4). Continuous irradiation was used in the preliminary test to provide a controlled reference condition for exposure time selection before evaluating modulation frequency effects *in vivo*.

Under modulated conditions, the accumulated dose remained constant for each fruit type (papaya: 0.66 kJ m^{-2}; orange: 0.99 kJ m^{-2}), while continuous irradiation resulted in approximately double the accumulated dose (papaya: 1.33 kJ m^{-2}; orange: 1.99 kJ m^{-2}) (Table 1). Differences in dose between papaya and orange resulted from the number of lamps used in each fruit (two lamps for papaya and three lamps for orange).

2.5.2.2. Experiment 2 (P2 and O2): effect of modulation frequency × exposure time. Experiments P2 and O2 evaluated combinations of two modulation frequencies and three exposure times, resulting in six UV-C treatments plus a control. This configuration represents a 2 × 3 factorial arrangement with an additional control treatment (Table 2). The selected frequencies and exposure times were defined based on the *in vivo* experiments P1 and O1, which identified treatment ranges that reduced anthracnose incidence and severity in papaya and sour rot in orange, while minimizing epidermal injury.

Exposure time determined the accumulated energy, with doses ranging from 0.33 to 1.33 kJ m^{-2} for papaya and from 0.99 to 5.97 kJ m^{-2} for orange (Table 2). Experiments were conducted in a CRD with six replicates per treatment in both papaya and orange fruits. Each experiment (P2 and O2) was performed twice, using different batches of fruit under the same experimental conditions.

Sample sizes differed across experiments (P1, O1, P2, and O2), because each experiment was conducted and analyzed independently.

2.5.2.3. Post-treatment storage and evaluations. After UV-C treatment,

Table 1
Characteristics of UV-C radiation for each treatment in the experiments P1 (papaya var. 'Papaia') and O1 (orange var. 'Lima'): $E_{T/2}$: energy delivered per semi-period; $N_{T/2}$: number of pulses per semi-period; t_{on}: exposure time; f_{ch}: modulation frequency. In continuous treatments (0 Hz), no pulses are generated, and $E_{T/2}$ and $N_{T/2}$ are not applicable.

Fruits	f_{ch} (Hz)	t_{on} (s)	$E_{T/2}$ (J m^{-2})	$N_{T/2}$	E_T Dose (kJ m^{-2})
Papaya	Control	-	-	-	0.00
	0	30	-	-	1.33
	15	30	1.47	450	0.66
	30	30	0.74	900	0.66
	45	30	0.49	1350	0.66
Orange	Control	-	-	-	0.00
	0	30	-	-	1.99
	15	30	2.21	450	0.99
	30	30	1.11	900	0.99
	45	30	0.74	1350	0.99

Control treatment consisted of fruit not exposed to UV-C radiation.

Table 2
Characteristics of UV-C radiation treatments in the experiments P2 (papaya var. 'Papaia') and O2 (orange var. 'Lima'): $E_{T/2}$: energy delivered per semi-period; $N_{T/2}$: number of pulses per semi-period; t_{on}: exposure time; f_{ch}: modulation frequency. In continuous treatments (0 Hz), no pulses are generated, and $E_{T/2}$ and $N_{T/2}$ are not applicable.

Fruits	f_{ch} (Hz)	t_{on} (s)	$E_{T/2}$ (J m^{-2})	$N_{T/2}$	E_T Dose (kJ m^{-2})
Papaya	Control	-	-	-	0.00
	0	15	-	-	0.66
	0	20	-	-	0.88
	0	30	-	-	1.33
	30	15	0.74	450	0.33
	30	20	0.74	600	0.44
	30	30	0.74	900	0.66
Orange	Control	-	-	-	0.00
	0	30	-	-	1.99
	0	60	-	-	3.98
	0	90	-	-	5.97
	45	30	0.74	1350	0.99
	45	60	0.74	2700	1.99
	45	90	0.74	4050	2.98

Control treatment consisted of fruit not exposed to UV-C radiation.

fruit were stored under controlled conditions suitable for symptom development: orange fruit at 26 ± 2 °C and 90 ± 2% RH for up to 13 days (experiments O1 and O2), and papaya fruit at 22 ± 2 °C and 90 ± 2% RH for up to 7 days (experiments P1 and P2).

For all experiments (P1, O1, P2, and O2), disease incidence, disease severity, incubation period, and possible UV-C–induced skin injury were evaluated daily for each fruit individually (P1 = 10 fruits per treatment, O1 = 8 fruits per treatment, and P2 and O2 = 6 fruits per treatment).

Incidence, a binary variable (presence/absence), was calculated using the percentage of fruits exhibiting visible disease symptoms on each evaluation day, and treatment effects were assessed based on final incidence. The incubation period was defined as the number of days between pathogen inoculation and the appearance of the first lesions. Disease severity was quantified by the mean lesion diameter, obtained from two orthogonal measurements, and used to construct the area under the disease progress curve (AUDPC) (Campbell and Madden, 1990).

The AUDPC for each fruit j under treatment k is calculated as the sum of the $(n-1)$ areas under the successive curve segments $(Y_{ijk}, Y_{(i+1)jk})$ corresponding to consecutive evaluation times (t_i, t_{i+1}). Each partial area is obtained by multiplying the mean of the two successive observations, $(Y_{ijk}, Y_{(i+1)jk})/2$, by the respective time interval (t_i+1, t_i), as described in Eq. 6.

$$AUDPC_{jk} = \sum_{i=1}^{n-1}\left[\left(\frac{Y_{ijk}+Y_{(i+1)jk}}{2}\right)\times\left(t_{(i+1)jk}-t_{ijk}\right)\right] \quad (6)$$

In Eq. 6, $AUDPC_{jk}$ is the area under the disease progress curve for replicate (fruit) j ($j = 1, 2, 3, \ldots n_j$) and treatment k ($k = 1, 2, \ldots, n_k$); Y_{ijk} is the mean lesion diameter (mm), calculated as the means of two orthogonal measurements, for replicate j under treatment k, at evaluation time i ($i = 1,2, \ldots, n_i$). Accordingly, the values of n_k were 5 for experiments P1 and O1, and 7 for experiments P2 and O2; the values of n_i (number of fruits used per treatment) were 10, 8, 6, and 6 in experiments P1, O1, P2, and O2, respectively.

Skin burn severity was assessed using a visual scale from 0 to 4 based on the intensity of damage observed on the fruit surface: 0 (no burn), 1 (almost imperceptible), 2 (slightly visible), 3 (visible), and 4 (intense). This scale allowed monitoring of burn severity throughout the storage period (the duration of the experiment). Fig. 1 shows burn level categories used to assess papaya fruit. The orange fruit, however, showed no visible signs of burning.

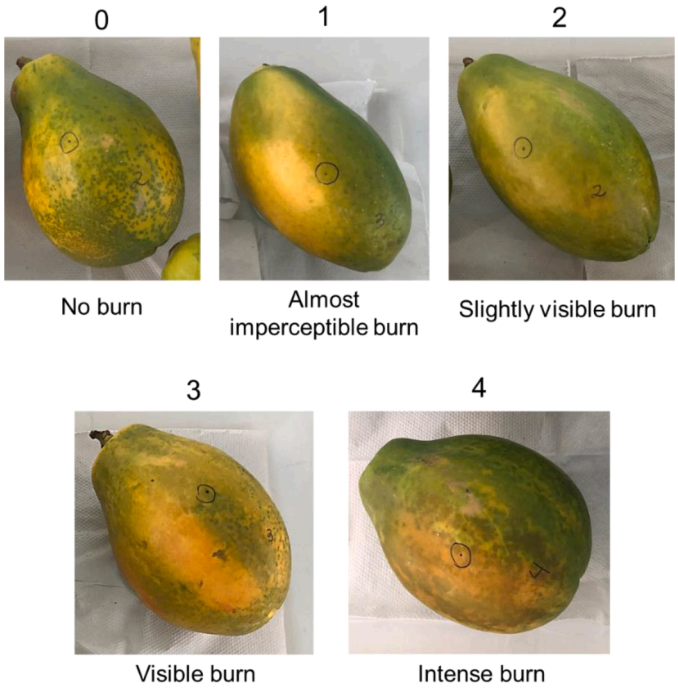

Fig. 1. Visual scale representing epidermal burn levels in papaya var. 'Papaia' fruit treated with UV-C radiation, ranging from 0 (no burn) to 4 (intense burn). The classification was defined based on the intensity of lesions observed on the fruit surface.

2.6. Experiment to evaluate the effect of UV-C radiation on fruit quality

In this experiment, two treatments were evaluated: control (non-irradiated) and UV-C irradiation of fruits. Orange fruit received a dose of 1.99 kJ m^{-2} (0 Hz/30 s), while papaya fruit received 0.44 kJ m^{-2} (30 Hz/20 s). These doses were defined based on the results of the previous *in vivo* experiments (P1, O1, P2, and O2), as they did not cause epidermal injury and reduced the incidence and severity of anthracnose and sour rot. The experimental design was a CRD, with 10 fruit per treatment for orange at each evaluation date and 5 fruit per treatment for papaya.

The papaya and orange fruits were washed with water and neutral detergent, dried using paper towels, and were not artificially inoculated with the pathogen. The fruits were then subjected to their respective UV-C treatments and stored at 20 ± 2 °C and 80 ± 2% RH, to simulate marketing conditions. Orange fruit was evaluated after 2, 6, and 8 days of storage, while papaya fruit was evaluated after 1, 3, and 6 days.

Weight loss (WL) was expressed as a percentage of the initial weight (Mohamed et al., 2017). Peel color was determined on opposite sides of each fruit using a colorimeter (CM-700d, Konica Minolta), in the CIE Lab* system (illuminant D65, 10° observer angle). Chroma (c*) and hue angle (h*) were calculated from the a* and b* values (Pathare et al., 2013).

Firmness was measured using a texture analyzer (TA500, Lloyd Instruments). For orange, equatorial compression was performed using a 490 N load cell, a 75-mm plate probe, 5% deformation, and a speed of 1 mm s^{-1} (Cháfer et al., 2012). For papaya, equatorial penetration on opposite sides was performed using a 500 N load cell, a 6 mm cylindrical probe, a 5 mm penetration depth, and a speed of 1 mm s^{-1} (Miranda et al., 2022). Force was expressed in Newtons (N).

Papaya juice was obtained by manual pressing of the pulp, while orange juice was extracted using a manual hand press; both juices were subsequently filtered through cheesecloth. Soluble solids (SS) were measured with a digital refractometer (MA871, Milwaukee Instruments) and expressed in °Brix. Titratable acidity (TA) was determined by

titrating 5 mL of juice diluted in 45 mL of distilled water with 0.1 N NaOH (Labsynth, 99% purity), standardized with Potassium Biphthalate (Vetec, 99.5% purity) and correction factor 0.86, to pH 8.1, and expressed as % citric acid (Equation 312/IV, Instituto., 2008). The SS/TA ratio was calculated as the direct ratio between SS and TA. pH was measured using a benchtop pH meter (2500, Cole-Parmer).

2.7. Experiment to evaluate the effect of UV-C radiation on fruit enzymatic activity

The UV-C doses and storage conditions were the same as those described in 2.6. However, to avoid possible detergent interference with enzymatic activity, fruits were washed only with running water before treatment. The Fruits were assigned to two treatments: non-irradiated control and UV-C-treated fruits.

The experimental design was a CRD, with four replicates (fruits) per treatment at each sampling time, using different fruits for each evaluation date. Fruits were not artificially inoculated with pathogens. Peel samples were collected at time zero, 2 h after treatment, and daily for six days.

2.7.1. Preparation of the enzyme extract

To prepare the enzyme extract, 1 g of peel obtained using a cork borer (8 mm diameter × 2 mm depth) was ground in liquid nitrogen and homogenized with 6 mL of 50 mM sodium phosphate buffer (pH 6.5) (Na_2HPO_4, CAS 7558–79–4 + $NaH_2PO_4{\cdot}H_2O$, CAS 10049–21–5, Sigma-Aldrich, Germany), containing 1% polyvinylpyrrolidone (PVP-10, CAS 9003–39–8, Sigma-Aldrich) and one mM phenylmethanesulfonyl fluoride (CAS 329–98–6, Sigma-Aldrich). The mixture was centrifuged at 20,000 × g for 25 min at 4 °C (Rotina 380, Andreas Hettich), and the supernatant was stored at –18 °C until analysis (Baracat-Pereira et al., 2001).

2.7.2. Determination of protein concentration

Protein concentration was determined according to Bradford (1976), by mixing 15 μL of the enzyme extract with 200 μL of Bradford reagent (B6916, 0.1–1.4 μg mL^{-1} protein, Sigma-Aldrich) and measuring absorbance at 595 nm between 2 and 10 min after reaction onset. Quantification was performed using a standard curve built with bovine serum albumin (BSA, 98% purity, CAS 9048–46–8, Sigma-Aldrich). Results were expressed as mg protein per g fresh tissue (mg protein g^{-1} fresh tissue). These data were used to calculate enzymatic activities in subsequent analyses.

2.7.3. Determination of enzymatic activity

2.7.3.1. Peroxidase. Peroxidase activity was determined using a reaction mixture consisting of 50 μL of extract, 72 μL of 10 mM sodium phosphate buffer (pH 6.5), 72 μL of 3 mM hydrogen peroxide (H_2O_2, 6% solution, CAS 7722–84–1, Scharlau), and 72 μL of 15 mM guaiacol (CAS 90–05–1, Sigma-Aldrich). Absorbance at 470 nm was monitored at 30 °C for three 20-second cycles (Hammerschmidt et al., 1982). One unit of activity (U) was defined as an increase of 0.01 absorbance units per minute. Enzyme activity was expressed as U mg^{-1} protein.

2.7.3.2. Polyphenoloxidase. Polyphenoloxidase activity was quantified using 20 μL of extract and 200 μL of 20 mM pyrocatechol (CAS 120–80–9, Exodo Científica) in 100 mM phosphate buffer (pH 6.8), with readings at 420 nm for four cycles of 30 s at 30 °C (Terao et al., 2017). One unit of activity (U) was defined as an absorbance change of 0.01 per minute. Results were expressed as U mg^{-1} protein.

2.7.3.3. Catalase. The reaction contained 140 μL of enzyme extract and 70 μL of 10 mM hydrogen peroxide in 50 mM phosphate buffer (pH 7.0), with absorbance readings at 240 nm for five cycles of 5 s at 25 °C (Aebi, 1984). Activity was calculated from the change in absorbance over time using the Lambert-Beer law ($A = \varepsilon{\cdot}b{\cdot}c$), where $\varepsilon = 39.4\ M^{-1}\cdot cm^{-1}$ is the molar extinction coefficient of H_2O_2, and b = 0.62 cm corresponds to the estimated optical path length of the microplate well. Results were expressed as μmol H_2O_2 decomposed per minute per milligram protein (μmol H_2O_2 min^{-1} mg^{-1} protein).

2.7.3.4. Phenylalanine Ammonia-Lyase. The activity was determined using 20 μL of extract, 90 μL of 100 mM borate buffer (pH 8.8) (H_3BO_3, CAS 10043–35–3, Sigma-Aldrich + $K_2B_4O_7{\cdot}4H_2O$, CAS 12045–78–2, Sigma-Aldrich), and 90 μL of 12 mM L-phenylalanine (CAS 63–91–2, Exodo Científica), incubated for 20 min at 37 °C (Pascholati et al., 1986). The reaction was stopped by adding 15 μL of 6 N HCl (37%, CAS 7647–01–0, Scharlau), and the trans-cinnamic acid formed was quantified at 290 nm using a standard curve. Results were expressed as μg min^{-1} mg^{-1} protein. The mass of potassium tetraborate tetrahydrate ($K_2B_4O_7{\cdot}4H_2O$) added was calculated based on the boron content of the compound. The molar mass of the salt was divided by 4 to correspond to the amount equivalent to 1 mol of boron.

Absorbance readings were performed in 96-well transparent microplates (655180, Greiner Bio-One) using a UV-Vis microplate spectrophotometer (Infinite 200 PRO, Tecan) and Magellan software version 7.2.

2.8. Statistical analysis

2.8.1. Evaluation of the photothermal effect

Temperature variation (°C) as a function of time (minutes) was described using a linear regression model fitted separately for each modulation frequency (0, 15, 30, and 45 Hz) (Eq. 7):

$$T_i = \beta_0 + \beta_1 . t + \varepsilon_i \quad (7)$$

In which, T_i represents the temperature observed in repetition i ($i = 1, 2, 3 \ldots 15$) for a given modulation frequency; β_0 and β_1 correspond to the model parameters, namely the intercept (estimated initial temperature) and slope (rate of temperature change per unit of time, °C min^{-1}), respectively. ε_i denotes the random error associated with T_i.

Model fitting was performed in R software version 4.5.3 (R Core Team, 2025) using the *lm* function from the *stats* package. For each frequency, the statistical significance of the coefficients was assessed using the *t*-test, and R^2 values were reported to express the proportion of variability explained by the model.

2.8.2. Evaluation of disease progress, fruit quality, and defense induction

Disease incidence was evaluated using Fisher's exact test (one-sided, lower-tailed) (Fisher, 1922) to compare each UV-C treatment with the control (no radiation). A one-sided test was used because the incidence under UV-C treatments is expected to be lower than in the control. In the present experiments, chi-square tests were considered inappropriate because some cells (treatment x disease presence combinations) had absolute frequencies below 5, necessitating Fisher's exact tests as an adequate alternative.

For severity data and mean incubation period in papaya experiments (P1 and P2), in which no treatment exhibited zero variance, analyses of variance were performed using the GLM procedure in SAS software version 9.4 (SAS/STAT, 2017, 2016). In experiment P1, contrasts between means corresponding of each modulation frequency treatment and the control mean were defined a priori and evaluated using *t*-tests for contrasts. For mean incubation period, upper-tailed *t*-tests were used because this period is expected to be higher for the UV-C treatments; conversely, for severity, the *t*-tests used were lower-tailed.

In experiments P2 and O2, where treatments correspond to combinations of modulation frequency and exposure time, firstly, the interaction between these factors was evaluated. Contrasts were defined based on the presence or absence of a significant interaction. In P2,

contrasts were evaluated using *t*-tests via the ESTIMATE statement of the GLM procedure (SAS/STAT, 2017, 2016). In O2 (which included treatments with zero variance), interactions and contrasts were assessed using the *nparcomp* R package (Konietschke et al., 2015), with contrast matrices specified using type = *"userdefined"*.

Burn injury data were analyzed using a one-sided (upper-tailed) nonparametric Dunnett test to compare the control mean with each UV-C treatment. The *nparcomp* package was used with type = *"dunnett"* and alternative = *"less"*, given the expectation that mean burn severity would always be greater in UV-C treatments than in the control.

For physicochemical and enzymatic analyses, homogeneity of variances between treatments was assessed using Levene's test (Levene, 1960). When homoscedasticity was not rejected, comparisons between treatments (control vs. UV-C) were performed using Student's *t*-test (Student, 1908) for independent samples assuming equal variances. Otherwise, the *t*-test for unequal variances was used.

A significance level of 0.05 was adopted for all statistical analyses.

3. Results

3.1. Photothermal effect

Temperature increase (°C) exhibited a linear relationship with exposure time at modulation frequencies used: 0, 15, 30, and 45 Hz (Fig. 2). The fitted linear regression models adequately described this relationship, with high coefficients of determination ($R^2 \geq 0.96$) for all frequencies. The heating rate (slope) was highest under continuous radiation (0 Hz: 0.65 °C min^{-1}) and progressively decreased with increasing frequency: 15 Hz = 0.54 °C min^{-1} ; 30 Hz = 0.47 °C min^{-1} ; 45 Hz = 0.35 °C min^{-1} (Table 3; Fig. 2).

3.2. Experiments P1 and O1 – Effect of continuous and modulated UV-C radiation under a constant exposure time on papaya and orange fruits

At the end of the evaluation period, UV-C treatments at 0 Hz and 30 Hz reduced anthracnose incidence in papaya fruit by 81% and 71%, respectively (Table 4). Both treatments also delayed lesion development, reducing the mean diameter and AUDPC values and prolonging the incubation period by 1.8 days compared to the control (Table 5; Table S2). The disease progress curves illustrate the slower increase in lesion diameter over time under these treatments (Fig. 3a).

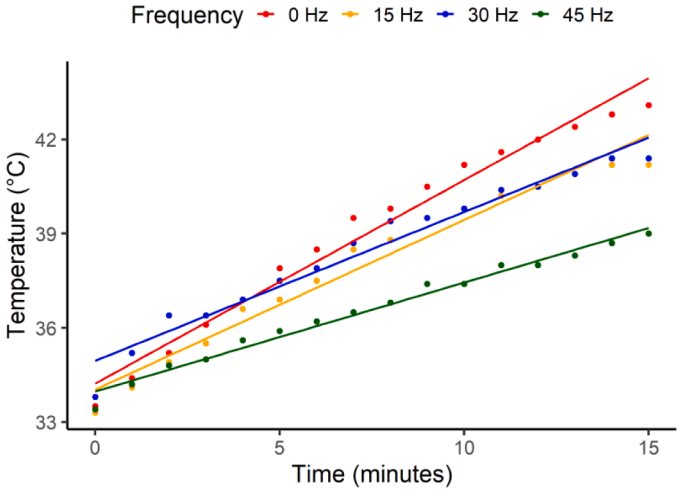

Fig. 2. Variation of the irradiation chamber temperature (°C) inside the UV-C system as a function of exposure time under different modulation frequencies (0, 15, 30, and 45 Hz). Fitted equations: 0 Hz: T = 34.22 + 0.65·Time (R^2 = 0.98); 15 Hz: T = 34.03 + 0.54·Time (R^2 = 0.97); 30 Hz: T = 34.95 + 0.47·Time (R^2 = 0.96); 45 Hz: T = 33.97 + 0.35·Time (R^2 = 0.98). The nominal significance level for the *t*-test of the slope was less than 0.001 for all models.

Table 3
Estimated parameters of linear regression models describing the relationship between irradiation chamber temperature inside the UV-C system and exposure time at modulation frequencies of 0 (continuous), 15, 30, and 45 Hz.

Frequency (Hz)	Model parameter	Estimate	SE[(1)]	t value	p-value[(2)]	R^2 [(3)]
0	Intercept	34.22	0.24	144.87	< 0.001	0.98
	Slope	0.65	0.03	24.18	< 0.001	
15	Intercept	34.03	0.23	145.73	< 0.001	0.97
	Slope	0.54	0.03	20.39	< 0.001	
30	Intercept	34.95	0.22	158.82	< 0.001	0.96
	Slope	0.47	0.02	18.97	< 0.001	
45	Intercept	33.97	0.11	312.10	< 0.001	0.98
	Slope	0.35	0.01	28.095	< 0.001	

Intercept and slope represent, respectively, the estimated initial temperature (°C) and the rate of temperature change (°C min^{-1}). [(1)] Standard error of each parameter estimate; [(2)] Nominal *t*-test p-value for each parameter; [(3)] Coefficient of determination: proportion of total variability explained by the model; p-value < 0.05 for the slope (highlighted in red) indicates a significant effect of exposure time on temperature.

For oranges, continuous UV-C (0 Hz) completely suppressed sour rot development (100%), while 45 Hz achieved an 80% reduction (Table 4). Both treatments significantly reduced disease severity and AUDPC compared with the control, with no significant effect on incubation period (Table 5, Table S3). This behavior is also reflected in the disease progress curves, where treated fruits showed a marked reduction in lesion progress compared to the control (Fig. 3b).

Regarding UV-C burns, no visible injury was observed in orange at any of the tested frequencies (Figure S5). In papaya, the continuous treatment (0 Hz) exhibited the highest burn rating (3.20), characterized by visible-to-intense burn areas (Table 6). In contrast, modulation frequencies of 15, 30, and 45 Hz resulted in milder levels of damage (1.60 and 1.80), corresponding to almost imperceptible to slightly visible burns (Table 6, Figure S6).

3.3. Experiments P2 and O2 – effect of modulation frequency × exposure time

In papaya fruit, the 30 Hz/20 s treatment showed the most pronounced effect (Table 7), reducing the incidence of anthracnose by 67% compared to the control (Table 7). No significant interaction was observed between modulation frequency and exposure time for any disease severity variable (MLD at day 7, AUDPC, and incubation period) (Table 8). The disease progress curves confirm this result, showing similar lesion development patterns across exposure times for both continuous and modulated treatments (Fig. 4a). Consequently, the effect of frequency (0 vs. 30 Hz) was consistent across all exposure times (15, 20, and 30 s), with no significant differences between continuous and modulated UV-C (Table 8).

When the control was compared to the overall mean of the UV-C treatments (Table 8), the irradiated fruit showed an 8.62 mm reduction in MLD and an increase of 1.28-day increase in the incubation period, confirming the effectiveness of UV-C in reducing anthracnose severity and delaying symptom onset in papaya fruit (Table 8).

Exposure to UV-C radiation caused varying levels of injury in papaya depending on exposure frequency and duration (Table 9). Fruits irradiated at 0 Hz showed more severe burns, especially at 20 and 30 s, with mean scores above 3.5. In contrast, modulation at 30 Hz for 20 s resulted in only mild injury (mean score 1.50), corresponding to nearly imperceptible to slightly visible damage.

In orange fruits, the 0 Hz/30 s treatment completely reduced the incidence of sour rot (100%; Table 7). No significant interaction was detected between UV-C frequency and exposure time for any of the variables related to sour rot severity in orange fruit (MLD at day 13, AUDPC and incubation period) indicating that the effect of modulation

Table 4
Disease incidence and reduction in incidence (%) in papaya and orange subjected to different UV-C radiation treatments were evaluated seven days (papaya) and thirteen days (orange) after treatment.

Fruits	UV-C treatment (frequency/time)	Dose (kJ m^{-2})	Number of fruits		Disease incidence[(1)] (%)	Incidence SE[(2)]	Incidence reduction (%)
			Infected	Not infected			
Papaya	Control	0.00	7	3	70	14.50	-
	0 Hz/30 s	1.33	1	9	10*	9.50	81
	15 Hz/30 s	0.66	5	5	50	15.80	29
	30 Hz/30 s	0.66	2	8	20*	12.60	71
	45 Hz/30 s	0.66	6	4	60	15.50	14
Orange	Control	0.00	5	3	62	17.10	-
	0 Hz/30 s	1.99	0	8	0*	0.00	100
	15 Hz/30 s	0.99	3	5	37	17.10	40
	30 Hz/30 s	0.99	2	6	25	15.30	60
	45 Hz/30 s	0.99	1	7	12	11.70	80

[(1)] Disease Incidence estimates followed by * differ from the control (no UV-C radiation) according to the lower-tailed Fisher's exact test at 0.05 significance level (n = 10 fruit per treatment for papaya and 8 fruit for orange).; [(2)] Standard error of the estimated percentage of infected fruits (incidence).

Table 5
Experiment P1 (papaya) and O1 (orange): Estimated treatment means (control and four UV-C frequencies) and their respective standard errors (SE) for anthracnose severity in papaya fruit and sour rot severity in orange fruit. Disease severity was expressed as the mean lesion diameter (MLD) at 7 days (papaya) and at 13 days after inoculation (orange), the area under the disease severity progress curve (AUDPC), and the incubation period (days).

Fruits	Treatment (UV-C emission frequency)	MLD (mm)		AUDPC (mm.day^{-1})		Incubation period (days)	
		Mean	SE*	Mean	SE*	Mean *	SE*
Papaya	Control	10.55	2.60	19.15	5.16	4.80	0.51
	0 Hz	01.98 *	2.60	03.66*	5.16	6.60*	0.51
	15 Hz	07.47	2.60	13.24	5.16	5.40	0.51
	30 Hz	02.70 *	2.60	04.11*	5.16	6.60*	0.51
	45 Hz	10.10	2.60	17.33	5.16	5.10	0.51
Orange	Control	28.24	12.40	149.41	70.80	08.50	01.57
	0 Hz	00.00 *	00.00	00.00*	00.00	13.00	00.00
	15 Hz	07.84 *	04.03	28.22*	14.69	10.88	01.04
	30 Hz	16.51 *	10.82	91.47*	59.97	10.63	01.56
	45 Hz	03.61 *	03.61	12.32*	12.32	12.25	00.75

* The standard errors of the mean estimates for all response variables are the same for all treatments because the hypotheses of homogeneous variances were not rejected. Asterisks (*) indicate a significant difference between each treatment and the control according to the lower one-tailed *t*-test for contrasts (n = 10 fruit per treatment for papaya and 8 fruit for orange).

(continuous vs. 45 Hz) did not vary across exposure times (30, 60, and 90 s) (Table 10). This is also evident in the disease progress curves, which show similar lesion development patterns among treatments (Fig. 4b).

Direct comparisons between continuous and modulated treatments also revealed no significant differences for any severity variable, regardless of exposure time (Table 10). Similarly, the contrasts between the control and the overall mean of UV-C treatments were not significant (Table 10). No burn symptoms were observed in the orange fruit at any of the frequencies tested.

Therefore, in subsequent assays evaluating the effect of radiation on quality attributes and enzymatic activities, the selected treatments were 0 Hz/30 s (1.99 kJ m^{-2}) for orange and 30 Hz/20 s (0.44 kJ m^{-2}) for papaya.

3.4. Effect of UV-C radiation on the postharvest quality of papaya and orange fruits

In papaya, modulated UV-C radiation at a dose of 0.44 kJ m^{-2} at 30 Hz/20 s contributed to firmness retention during the first three days of storage and delayed color change, thereby maintaining the green peel coloration for a longer period. No significant changes were observed in soluble solids (SS), titratable acidity (TA), or the SS/TA ratio. The pH values were slightly lower in irradiated fruit, with a slight increase only on the 6th day of storage. Mass loss progressed similarly for both treatments throughout storage (Tables 11 and 12, Figure S8).

In orange, continuous UV-C radiation at a dose of 1.99 kJ m^{-2} at 0 Hz/30 s produced a more persistent effect. Irradiated fruit maintained higher firmness up to the 6th day of storage (22.58 N vs. 18.83 N in the control). No relevant changes were observed in TA. However, irradiated fruit exhibited a slight increase in pH and a reduction in SS at the end of storage (pH 5.13 vs. 5.11 in the control; SS 8.22 °Brix vs. 9.27 °Brix in the control), resulting in a lower SS/TA ratio. Regarding peel color, UV-C radiation enhanced orange pigmentation, as indicated by a reduction in the hue angle (h*) with no significant effect on lightness (L*) (Tables 11 and 12, Figure S9).

3.5. Effect of UV-C radiation on the enzymatic activity of papaya and orange fruits

UV-C radiation stimulated the activity of antioxidant (catalase and peroxidase) and defense-related enzymes (phenylalanine ammonia-lyase and polyphenol oxidase), with rapid responses during the first hours following treatment (Figure S10 and S11).

The activity of phenylalanine ammonia-lyase in papaya fruit exhibited a sharp increase 2 h after UV-C treatment, followed by a gradual decline until the end of the experimental period. In orange fruit, phenylalanine ammonia-lyase showed a significant difference between the UV-C treatment and the control only on day 3, when UV-C resulted in higher activity. For both fruits, enzymatic levels were similar between treatments on the sixth day of evaluation (Fig. 5, Table S4).

Polyphenoloxidase in papaya fruit exhibited a pronounced peak 2 h after UV-C treatment, significantly higher than in the control. In the subsequent days, the control fruit maintained low and stable activity, whereas UV-C treated fruit showed fluctuations, with additional peaks on days 2, 4, and 6, although these were not statistical significance at those time points. In orange fruit, both treatments exhibited similar temporal patterns, with no significant differences (Fig. 5, Table S5).

For peroxidase, papaya fruit showed higher initial activity in UV-C-treated fruit, followed by oscillations from day 2 onward. In orange fruit, however, significant differences were observed on days 1 and 3, when UV-C treatment resulted in higher peroxidase activity compared with the control (Fig. 6, Table S6).

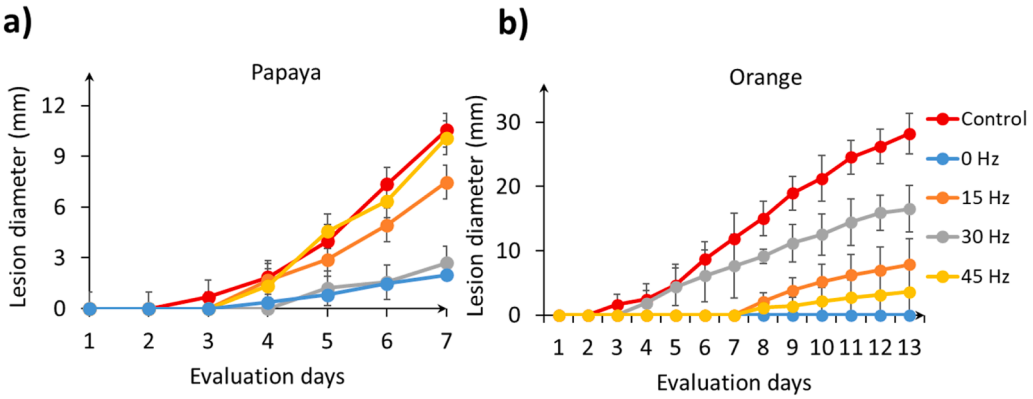

Fig. 3. Disease progress curves calculated from severity expressed as mean lesion diameter: (a) anthracnose in papaya caused by *Colletotrichum gloeosporioides*, and (b) sour rot in orange caused by *Geotrichum citri-aurantii*. Vertical bars on the lines represent the standard error.

Table 6
Mean and standard error (SE) of burn severity in papaya fruit exposed to continuous UV-C radiation (0 Hz/30 s, 1.33 kJ m^{-2}) and modulated UV-C radiation (15, 30, and 45 Hz/30 s, 0.66 kJ m^{-2}), with corresponding visual descriptions.

UV-C treatment (frequency/time)	Mean	SE	Visual description
Control	0.00	0.00	No burn
0 Hz/30 s	3.20*	0.13	Visible to intense
15 Hz/30 s	1.80*	0.18	Almost imperceptible to slightly visible
30 Hz/30 s	1.80*	0.13	Almost imperceptible to slightly visible
45 Hz/30 s	1.60*	0.16	Almost imperceptible to slightly visible

Burn severity rating scale: 0 = no burn; 1 = almost imperceptible burn; 2 = slightly visible burn; 3 = visible burn; 4 = intense burn. Means followed by * indicate statistically significant differences among treatments ($p < 0.05$; Dunnett's nonparametric test, n = 10).

Catalase exhibited contrasting responses between the fruit species. In papaya, activity remained consistently higher in treated fruit throughout storage, with pronounced peaks at 2 h and again at 2 days after treatment. In orange, control fruit maintained low activity, whereas irradiated fruit showed a sharp peak 2 h after treatment and again on the 5th day, followed by a decline, resulting in similar levels between treatments at the end of the evaluation period (Fig. 6, Table S7).

4. Discussion

Modulation of UV-C radiation may influence the efficacy of postharvest treatment. In the present study, treatments were standardized by exposure time rather than total dose, so continuous and modulated applications received the same irradiation period. As a result, the total delivered dose varied across treatments, with modulated UV-C delivering lower doses. This occurs because, in modulated mode, the alternation between periods of light and absence of light reduces the total dose received by the fruit. Even under these conditions, similar levels of disease control were observed between continuous and modulated treatments, suggesting that modulation increased treatment efficiency.

In addition, differences in modulation frequency were associated with changes in energy delivery per pulse. Lower frequencies were associated with higher energy per pulse ($E_{T/2}$; Table 1), which was associated with greater thermal accumulation in the radiation chamber (Fig. 2). In contrast, higher frequencies distributed the delivered energy into a greater number of lower-intensity pulses, resulting in smaller temperature increases near the irradiated surface (Fig. 2). This inverse relationship between frequency and pulse energy suggests that modulation may also influence heat accumulation during UV-C exposure. These observations are consistent with findings highlighting the importance of energy-delivery dynamics for optimizing both tissue safety and germicidal efficiency (Armagan and Demirci, 2025).

Table 7
Disease incidence and reduction in incidence (%) in papaya and orange subjected to different combinations of UV-C radiation frequencies and exposition times, evaluated at seven days (papaya) and thirteen days (orange) after treatment.

Fruits	UV-C treatment (frequency/time)	Dose (kJ m^{-2})	Number of fruits		Disease incidence[(1)] (%)	Incidence SE[(2)]	Incidence reduction (%)
			Infected	Not infected			
Papaya	Control	0.00	6	0	100	0.00	-
	0 Hz/15 s	0.66	4	2	67	19.20	33
	0 Hz/20 s	0.88	3	3	50	20.40	50
	0 Hz/30 s	1.33	5	1	83	15.20	17
	30 Hz/15 s	0.33	2	4	33*	19.20	67
	30 Hz/20 s	0.44	2	4	33*	19.20	67
	30 Hz/30 s	0.66	4	2	67	19.20	33
Orange	Control	0.00	3	3	50	20.40	-
	0 Hz/30 s	1.99	0	6	0*	0.00	100
	0 Hz/60 s	3.98	2	4	33	19.20	33
	0 Hz/90 s	5.97	3	3	50	20.40	00
	45 Hz/30 s	0.99	1	5	17	15.20	67
	45 Hz/60 s	1.99	1	5	17	15.20	67
	45 Hz/90 s	2.98	4	2	67	19.20	00

[(1)] Disease Incidence estimates followed by * differ from the control (no UV-C radiation) according to the lower-tailed Fisher's exact test at a 0.05 significance level; [(2)] Standard error of the estimated percentage of infected fruits (incidence).

Table 8
Experiment P2: Estimates of planned contrasts to investigate the interaction between UV-C frequency and exposure time (F x T), the overall effect of the modulation frequency 30 Hz compared to the continuous emission regardless of the exposure time (F0 x F30), and the overall influence of UV-C radiation on the anthracnose evolution in papaya fruit (control x UV-C). The response variables evaluated were disease severity expressed as the mean lesion diameter at the 7th day after inoculation (MLD), the area under the disease progress curve (AUDPC), and the disease incubation period (days).

Response variable	Contrast	Estimate	SE[(a)]	t-value	p-value[(b)]
MLD at the 7th day (mm)	Interaction T X F[(c)]	1.91	3.88	0.49	0.6249
	F0 x F30[(d)]	0.47	1.58	0.30	0.7682
	Control x UV-C[(d)]	8.62	2.24	3.85	0.0005
AUDPC (mm.day^{-1})	Interaction T X F[(c)]	1.59	3.03	0.52	0.6033
	F0 x F30[(d)]	-2.53	2.50	-1.01	0.1601
	Control x UV-C[(d)]	13.72	4.58	3.00	0.0050
Incubation period (days)	Interaction T X F[(c)]	0.00	0.98	0.00	1.0000
	F0 x F30[(e)]	0.00	0.40	0.00	1.0000
	Control x UV-C[(e)]	-1.28	0.53	-2.26	0.0299

[(a)] Standard error of the contrast estimate differences (SE); [(b)] nominal significance level associated with *t*-test for contrasts: [(c)] two-sided *t*-test, [(d)] upper-tailed *t*-test and [(e)] lower-tailed *t*-test. P-values highlighted in red ($p < 0.05$) indicate significant differences between groups of treatment means at a 0.05 significance level.

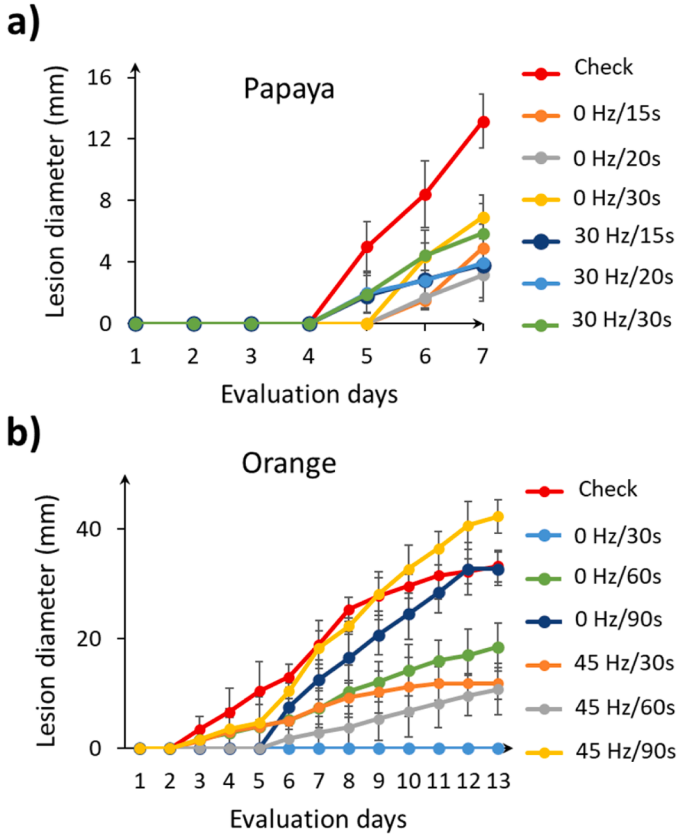

Fig. 4. Disease progress curves calculated from severity expressed as mean lesion diameter: (a) anthracnose in papaya caused by *Colletotrichum gloeosporioides*, and (b) sour rot in orange caused by *Geotrichum citri-aurantii*. Vertical bars on the lines represent the standard error.

Table 9
Estimated means and respective standard errors (SE) of burn severity scores in papaya fruit exposed to different combinations of UV-C radiation frequencies and exposition times, with corresponding visual description.

Treatment (frequency/time)	Dose (kJ m^{-2})	Mean	SE	Visual description
Control	0.00	0.00	0.00	No burn
0 Hz/15 s	0.66	2.67*	0.49	Slightly visible to visible burn
0 Hz/20 s	0.88	3.50*	0.34	Visible to intense burn
0 Hz/30 s	1.33	3.83*	0.17	Visible to intense burn
30 Hz/15 s	0.33	1.67*	0.42	Almost imperceptible to slightly visible burn
30 Hz/20 s	0.44	1.50*	0.34	Almost imperceptible to slightly visible burn
30 Hz/30 s	0.66	2.17*	0.17	Slightly visible burn

Burn severity scale: 0 = no burn; 1 = almost imperceptible burn; 2 = slightly visible burn; 3 = visible burn; 4 = intense burn. Means followed by * indicate statistically significant differences between the corresponding UV-C treatment and the control by the upper-tailed Dunnett's nonparametric test, n = 6 fruit per treatment).

However, it is important to note that the photothermal effect in this study was evaluated solely based on the temperature measured within the irradiation chamber, with the thermocouple positioned on a section of rigid expanded polystyrene (EPS) board, and no direct monitoring of the fruit surface temperature. Future investigations should include direct measurements of fruit surface temperature to more accurately characterize local heating effects and their implications for postharvest quality.

The different responses to UV-C treatments between papaya and orange can be explained by their distinct physiological characteristics, particularly their climacteric and non-climacteric behavior. In papaya, a climacteric fruit characterized by high metabolic activity and a relatively thin, sensitive epidermis, continuous-mode exposure (0 Hz) effectively controlled anthracnose, reducing disease incidence by around 50%; however, it also caused epidermal burns at longer exposure times, indicating thermal limitations of the tissue. UV-C treatments significantly reduced disease severity and AUDPC and delayed symptom onset by approximately 1.28 days, suggesting that disease suppression involved both direct antifungal effects and host defense responses.

In contrast, modulation at 30 Hz/20 s preserved surface integrity while providing disease suppression comparable to that of the continuous mode, even at half the dose (0.44 kJ m^{-2} modulated vs. 0.88 kJ m^{-2} continuous). This indicates that treatment effectiveness depends not only on total dose but also on the mode of energy delivery. Continuous exposure delivers uninterrupted radiation, which may intensify stress on the fruit surface and increase damage to both fungal and epidermal cells. In metabolically active fruits such as papaya, this sustained stress can exceed tissue tolerance, leading to injury. Conversely, modulated UV-C introduces brief pauses between pulses, allowing partial heat dissipation and reducing surface stress, thereby minimizing epidermal damage while maintaining antimicrobial activity.

In orange, a non-climacteric fruit, continuous UV-C treatment (0 Hz/30 s) completely suppressed sour rot (100%) without visible peel injury. The greater tolerance in orange can be attributed to both lower metabolic activity and the structural and biochemical properties of the peel (Yamaga and Hamasaki, 2020). The citrus flavedo acts as an effective physical barrier, limiting radiation penetration and reducing heat transfer to internal tissues (Ruiz et al., 2016). In addition, UV-C exposure can stimulate defense responses in the peel, including the accumulation of phytoalexins, polymethoxyflavones, and antioxidant compounds, enhancing resistance to microbial decay and oxidative stress (Yamaga and Hamasaki, 2020). On the other hand, papaya peel is generally more susceptible to UV-C-induced damage due to its thinner structure and higher metabolic activity (Fabi and Do Prado, 2019). This reduced protective capacity may allow greater penetration of radiation and heat

Table 10
Experiment O2: Estimates of planned contrasts to investigate interaction between UV-C frequency and exposure time (F x T), the overall effect of the modulation frequency 45 Hz compared to the continuous emission regardless of the exposure time (F0 x F45), and the difference between the overall median of UV-C treatments and the control median (control x UV-C). The response variables evaluated for sour rot evolution in orange fruit were: disease severity, expressed as the mean lesion diameter at the 13th day after inoculation (MLD); the area under the disease progress curve (AUDPC); and the disease incubation period (days).

Response variable	Contrast[1]	Estimate[2]	SE[3]	t-value	p-value[4]	Hypothesis type
MLD at the 13th day (mm)	Interaction F x T[5]	0.42	0.08	0.99	0.55519	two-sided
	Continuous x 45 Hz[5]	0.46	0.07	-0.49	0.6390	two-sided
	Control x UV-C[6]	0.60	0.21	1.00	0.8319	right-sided (upper-tailed)
AUDPC ($mm.day^{-1}$)	Interaction F x T[5]	0.41	0.08	-1.09	0.4989	two-sided
	Continuous x 45 Hz[5]	0.47	0.08	-0.41	0.6940	two-sided
	Control x UV-C[6]	0.65	0.14	1.06	0.1618	right-sided (upper-tailed)
Incubation period (days)	Interaction F x T[5]	0.59	0.08	1.09	0.4972	two-sided
	Continuous x 45 Hz[5]	0.53	0.07	0.47	0.6521	two-sided
	Control x UV-C[7]	0.35	0.14	-1.06	0.1611	left-sided (lower-tailed)

[1] Planned contrasts with [2] their respective contrast estimates and [3] standard errors (SE); [4] nominal significance level associated with the *t*-tests based on global pseudo-ranks; [5] two-sided *t*-test; [6] lower-tailed *t*-test and [7] upper-tailed *t*-test. Values highlighted in red indicate ($p < 0.05$) significant contrasts at the 0.05 significance level ($n = 6$ fruit per treatment).

Table 11
Estimated means (papaya, $n = 5$; orange, $n = 10$) of physicochemical parameters and their respective standard errors (SE) from fruit non-irradiated (control) or irradiated with UV-C (papaya, 30 Hz/20 s, dose 0.44 kJ m^{-2}; orange, 0 Hz/30 s, dose 1.99 kJ m^{-2}). The measurements were made after 1, 3, and 6 days of storage (papaya) and 2, 6, and 8 days of storage (orange) at 20 ± 2 °C and 80 ± 2% relative humidity. Firmness (F, Newton), pH, soluble solids (SS, °Brix), titratable acidity (TA, %), SS/TA ratio, and weight loss (WL, %).

Response	Fruits	Treatment	1st measurement			2nd measurement			3rd meausrement		
			Mean	SE[1]	p[2]	Mean	SE[1]	p[2]	Mean	SE[1]	p[2]
F (N)	Papaya	Control	9.72	2.58	0.0002	10.38	3.09	0.0005	10.27	**4.78**	0.6761
		UV-C	33.71	2.58		34.57	3.09		4.43	**0.49**	
	Orange	Control	23.27	1.00	0.4135	18.83	**0.44**	0.1209	18.69	0.85	0.2946
		UV-C	22.08	1.00		22.58	**1.46**		17.40	0.85	
pH	Papaya	Control	5.36	0.05	0.0007	5.22	0.09	0.4349	5.32	0.04	0.0216
		UV-C	4.98	0.05		5.12	0.09		5.14	0.04	
	Orange	Control	5.14	0.02	0.0004	5.10	0.03	0.0145	5.11	**0.01**	0.3458
		UV-C	5.24	0.02		5.21	0.03		5.13	**0.02**	
SS (°Brix)	Papaya	Control	10.02	0.27	0.8404	10.58	0.30	0.1383	10.04	0.23	0.6835
		UV-C	9.94	0.27		9.88	0.30		9.90	0.23	
	Orange	Control	9.15	0.26	0.3112	9.24	0.34	0.8364	9.27	0.25	0.0082
		UV-C	8.76	0.26		9.14	0.34		8.22	0.25	
TA (%)	Papaya	Control	0.03	0.00	1.0000	0.03	**0.00**	0.1770	0.03	0.00	0.1822
		UV-C	0.03	0.00		0.03	**0.01**		0.03	0.00	
	Orange	Control	0.08	0.00	1.0000	0.08	0.00	0.0299	0.07	0.00	0.5598
		UV-C	0.08	0.00		0.07	0.00		0.07	0.00	
SS / TA	Papaya	Control	377.47	44.92	0.7850	412.85	31.12	0.6921	391.77	47.85	0.2858
		UV-C	359.55	44.92		430.92	31.12		314.38	47.85	
	Orange	Control	117.93	4.98	0.4577	114.89	5.29	0.1148	134.38	7.96	0.0860
		UV-C	112.58	4.98		127.30	5.29		113.95	7.96	
WL (%)	Papaya	Control	0.48	0.03	0.2673	0.94	0.07	0.2889	1.55	0.11	0.2072
		UV-C	0.53	0.03		1.05	0.07		1.76	0.11	
	Orange	Control	1.05	**0.01**	0.1358	2.45	**0.03**	0.1820	3.15	**0.04**	0.1820
		UV-C	0.98	**0.04**		2.28	**0.09**		2.93	**0.11**	

[1] Standard errors highlighted in blue indicate rejection of the variance homogeneity hypothesis according to Levene's test at a 0.05 significance level. [2] Nominal significance level (p-value) of the Student's *t*-test for independent samples. P-values highlighted in red, for each variable, indicate significant differences between treatment means.

transfer to underlying tissues, increasing the likelihood of physiological disorders and visible injury under continuous exposure (Fabi and Do Prado, 2019). The modulation may be important for papaya, as it can help maintain antifungal efficacy while reducing the risk of peel damage.

Furthermore, the slight temperature increase observed during continuous irradiation may have acted synergistically with UV-C in orange, enhancing pathogen inactivation without exceeding tissue tolerance. Previous studies have shown that UV-C efficacy depends not only on dose but also on treatment conditions such as temperature and irradiation regime (Baligad et al., 2023; Esua et al., 2020). The combination of mild heat stress and UV-C has been reported to increase pathogen sensitivity (Da Silva et al., 2023; Sripong et al., 2015), supporting the hypothesis that warming inside the irradiation chamber contributed to sour rot suppression in orange. Importantly, moderate temperature increases (3–4 °C) do not appear to compromise fruit quality (Santamera et al., 2020), suggesting that the thermal conditions observed here were within a safe range.

Consistent with these observations, longer exposure times did not improve disease suppression and, in papaya, were associated with an increased risk of thermal injury. Excessive heat generated during UV-C irradiation can lead to cellular damage, including membrane disorganization, increased oxidative stress, and metabolic alterations (Ullah et al., 2024). Therefore, selecting an appropriate combination of modulation frequency and exposure time is essential to achieve effective disease control while preserving epidermal integrity.

In terms of postharvest quality, papaya exhibited a rapid loss of firmness was in the control, as expected for climacteric fruit due to pectin degradation and cell wall disassembly (Kan et al., 2025; Pinto et al., 2011). In contrast, the modulated UV-C treatment (0.44 kJ m^{-2} at

Table 12
Estimated means (papaya, n = 5; orange, n = 10) of the color parameters L, a*, b*, c*, h* and their respective standard errors (SE) in fruit non-irradiated (control) or irradiated with UV-C (papaya, 30 Hz/20 s, dose 0.44 kJ m^{-2}; orange, 0 Hz/30 s, dose 1.99 kJ m^{-2}). The measurements were made after 1, 3, and 6 days of storage (papaya) and 2, 6, and 8 days of storage (orange) at 20 ± 2 °C and 80 ± 2% relative humidity.

Response	Fruits	Treatment	1st measurement			2nd measurement			3rd meausrement		
			Mean	SE[(1)]	p[(2)]	Mean	SE[(1)]	p[(2)]	Mean	SE[(1)]	p[(2)]
L*	Papaya	Control	49.23	1.32	0.8149	56.02	1.78	0.1704	60.02	0.89	0.1363
		UV-C	48.77	1.32		52.23	1.78		57.94	0.89	
	Orange	Control	57.50	**0.67**	0.7912	62.20	1.61	0.6102	65.10	1.31	0.9204
		UV-C	58.35	**1.67**		63.39	1.61		65.28	1.31	
a*	Papaya	Control	-6.61	0.79	0.2689	-1.77	1.10	0.0347	5.27	1.48	0.3779
		UV-C	-7.95	0.79		-5.75			3.31	1.48	
	Orange	Control	-5.40	**0.57**	0.5705	-1.84	1.21	0.1689	0.70	1.63	0.2899
		UV-C	-5.03	**1.30**		0.61	1.21		3.22	1.63	
b*	Papaya	Control	32.64	1.13	0.0740	39.42	2.45	0.2388	46.53	1.05	0.2012
		UV-C	29.34	1.13		35.01	2.45		44.46	1.05	
	Orange	Control	46.95	**0.86**	0.6229	44.26	2.17	0.9301	44.34	1.96	0.4684
		UV-C	47.43	**2.39**		43.98	2.17		42.28	1.96	
c*	Papaya	Control	33.37	1.06	0.0855	39.56	2.31	0.2624	46.99	1.19	0.2267
		UV-C	30.44	1.06		35.63	2.31		44.79	1.19	
	Orange	Control	47.36	**0.81**	0.6229	44.56	2.12	0.9076	44.53	2.00	0.5646
		UV-C	47.92	**2.29**		44.21	2.12		42.88	2.00	
h*	Papaya	Control	101.58	1.59	0.1416	92.76	2.24	0.0455	84.14	1.67	0.4938
		UV-C	105.24	1.59		100.24	2.24		85.83	1.67	
	Orange	Control	96.88	**0.79**	0.5202	93.30	1.77	0.2419	89.69	2.15	0.3526
		UV-C	96.83	**1.72**		90.28	1.77		86.79	2.15	

(1) Standard errors highlighted in blue indicate rejection of variance homogeneity hypothesis according to Levene's test at a 0.05 significance level. (2) Nominal significance level (p-value) of the Student's *t*-test for independent samples. P-values highlighted in red, for each variable, indicate significant differences between treatment means.

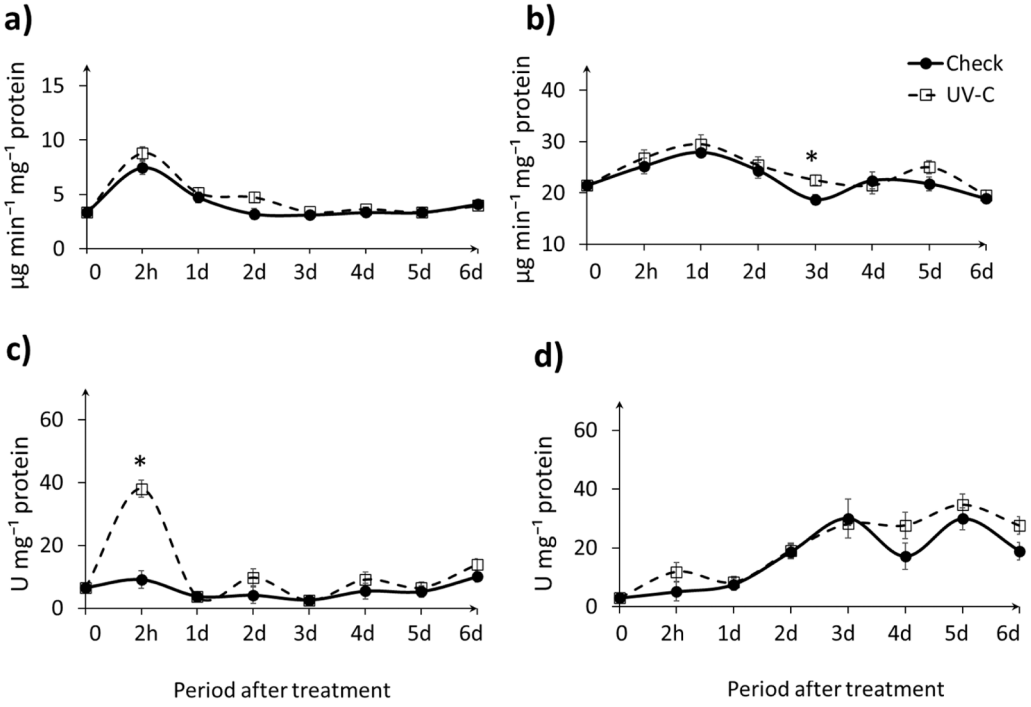

Fig. 5. Temporal pattern of the enzymatic activity of phenylalanine ammonia-lyase (a) papaya var. 'Papaia' and b) orange var. 'Lima') and polyphenoloxidase (c) papaya and d) orange) not treated (control) or treated with UV-C radiation (1.99 kJ m^{-2} (0 Hz/30 s) and 0.44 kJ m^{-2} (30 Hz/20 s) for orange and papaya, respectively). Fruits were stored at 20 ± 2 °C and 80 ± 2% relative humidity for up to 6 days. Samples were collected at fruit arrival (time zero), 2 h, and 1, 2, 3, 4, 5 and 6 days after treatment. (*) indicate significant differences between the control and the corresponding UV-C treatment means according to the Student's *t*-test for independent samples. Vertical bars represent standard errors of the respective mean estimates. One unit (U) corresponded to an increase of 0.01 in absorbance per minute (ΔAbs min^{-1}).

30 Hz/20 s) showed delayed softening during the early storage period. This response may be associated with reduced photothermal stress, which can limit membrane disruption and oxidative damage, thereby slowing down the activity of cell wall-degrading enzymes and preserving tissue structure (Kan et al., 2025). Similar effects have been reported in peaches treated with continuous UV-C at 4 kJ m^{-2} (Kan et al., 2025) and in guavas treated with 2 kJ m^{-2} (Menaka et al., 2024). However, this effect was not sustained throughout storage, likely due to the inherently high metabolic activity of climacteric fruits.

The maintenance of lower pH values in irradiated papaya fruit

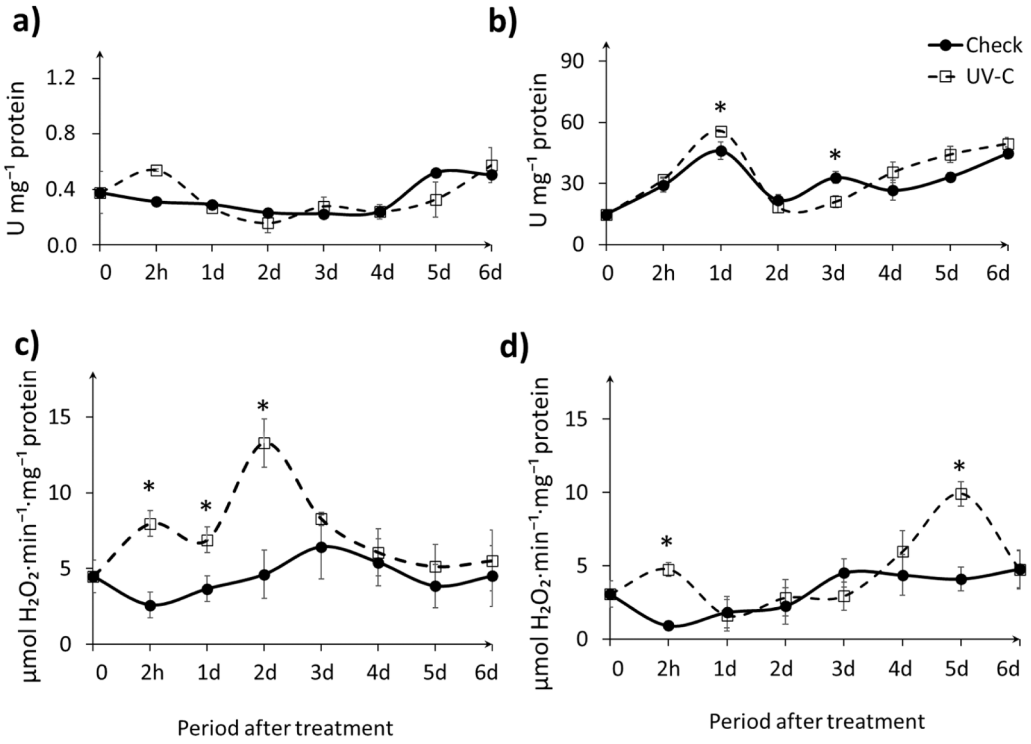

Fig. 6. Temporal pattern of the enzymatic activity of peroxidase (a) papaya var. 'Papaia' and, b) orange var. 'Lima') and catalase (c) papaya and d) orange) not treated (control) or treated with UV-C radiation (1.99 kJ m^{-2} (0 Hz/30 s) and 0.44 kJ m^{-2} (30 Hz/20 s) for orange and papaya, respectively). Fruits were stored at 20 ± 2 °C and 80 ± 2% relative humidity for up to 6 days. Samples were collected at fruit arrival (time zero), 2 h, and 1, 2, 3, 4, 5 and 6 days after treatment. (*) indicate significant differences between the control and the corresponding UV-C treatment means according to the Student's *t*-test for independent samples. Vertical bars represent standard errors of the respective mean estimates. One unit (U) corresponded to an increase of 0.01 in absorbance per minute (ΔAbs min^{-1}).

further supports this interpretation, indicating reduced metabolic activity and better retention of organic acids (Chitarra and Chitarra, 2005). These responses suggest that a lower thermal load during irradiation may have slowed metabolic processes associated with ripening and senescence. Similar stability in titratable acidity and pH has been reported in UV-C-treated peaches (Abdipour et al., 2019).

In orange, the effects of UV-C were more stable and persistent throughout storage. Firmness was maintained up to day 6, indicating preservation of cell wall integrity (Phonyiam et al., 2021). The lower weight loss observed in treated fruit may be associated with improved epidermal integrity and reduced transpiration (Menaka et al., 2024). In addition, UV-C has been reported to induce the formation of a thin protective surface layer that reduces water vapor diffusion (Abdipour et al., 2020), which may explain the reduced mass loss observed in the present study. The greater stability observed in orange may also be related to its higher tolerance to photothermal stress, due to structural characteristics of the peel (Ruiz et al., 2016). Regarding flavor attributes, only minor variations in soluble solids (SS) and the SS/TA ratio were observed, indicating minimal impact on sensory quality. This behavior is consistent with previous findings in citrus fruits (Acevedo-Daza et al., 2024; Pristijono et al., 2019).

Color, a critical parameter for commercial acceptance, responded according to the species-specific metabolic profile. UV-C radiation can affect the activity of enzymes involved in chlorophyll degradation and pigment biosynthesis (Castillejo et al., 2022; Hu et al., 2019). In papaya, smaller variations in a* and h* values suggest a slight delay in the loss of green coloration. In orange, the progressive increase in a* and decrease in h* reflect natural color intensification, a desirable commercial attribute. Similar responses have been reported in mangoes treated with continuous UV-C at 4 kJ m^{-2} (Pristijono et al., 2020) and in grapes treated with 2.4 kJ m^{-2} (Kuck and Noreña, 2021), indicating that UV-C, when applied within appropriate ranges, does not disrupt normal ripening-related color changes. Additionally, increases in L* and b* values, together with stability of c*, indicate that UV-C did not compromise color saturation but rather accompanied the natural ripening process. These results suggest that, under controlled photothermal conditions, UV-C preserves pigment metabolism and allows normal color development during ripening (Castillejo et al., 2022; Hu et al., 2019).

These findings demonstrate that the photothermal effect is a critical factor linking UV-C application to fruit quality. While excessive heat can accelerate tissue damage and loss of quality, controlled energy delivery, such as modulated UV-C, can reduce thermal stress, preserve cellular integrity, and maintain key quality attributes during storage.

Enzymatic results indicate that UV-C may act as a resistance inducer, as suggested by the rapid activation of defense-related enzymes. Immediately after irradiation, increases in the activity of phenylalanine ammonia-lyase, peroxidase, and polyphenoloxidase were observed, a pattern also described in strawberries and acerola (Erkan et al., 2008; Rabelo et al., 2020). This response is likely triggered by the generation of reactive oxygen species (ROS) in plant tissues upon UV-C exposure. These ROS act as signaling molecules, activating defense-related genes and initiating downstream biochemical pathways associated with stress responses (Kan et al., 2025).

The sharp increase in phenylalanine ammonia-lyase activity observed 2 h after treatment in papaya, as well as the later peak detected in orange on day 3, suggests activation of the phenylpropanoid pathway. This pathway leads to the synthesis of phenolic compounds, including flavonoids, phenolic acids, and lignin precursors, which are associated with enhanced resistance to pathogens and structural reinforcement of the cell wall (Deng and Lu, 2017). Under UV-C-induced stress, the upregulation of phenylalanine represents a key metabolic shift toward the accumulation of these protective compounds (Menaka et al., 2024). The prolonged maintenance of phenylalanine activity observed during storage in both fruits indicates that UV-C induces not only an immediate oxidative signal but also a prolonged activation of defense metabolism.

The increases in polyphenoloxidase and peroxidase activities further support the role of UV-C in strengthening plant defense mechanisms. These enzymes catalyze the oxidation and polymerization of phenolic compounds into quinones and lignin-like structures, contributing to cell wall reinforcement and the formation of antimicrobial barriers that limit pathogen development (Mayer, 2006; Passardi et al., 2004). This response is consistent with previous studies showing that polyphenoloxidase and peroxidase contribute to the formation of physical and chemical barriers against pathogens following abiotic stress (Purwar et al., 2012; Zou et al., 2025). In papaya, the early peak followed by sustained PPO activity suggests a rapid and continuous defense response, whereas in orange, the more stable enzymatic profile reflects the slower metabolic dynamics typical of non-climacteric fruits.

UV-C radiation also modulated the oxidative stress response. The increases in catalase and peroxidase activities after irradiation indicate activation of antioxidant defense mechanisms that regulate ROS levels. While moderate ROS accumulation pathways, excessive ROS can cause oxidative damage and accelerate senescence (Kan et al., 2025). In this context, catalase plays a central role by decomposing hydrogen peroxide (H_2O_2) into water and oxygen, thereby maintaining redox homeostasis and protecting cellular structures. The higher and more sustained catalase activity observed in papaya suggests a stronger antioxidant response, consistent with its higher metabolic activity and sensitivity to stress. In contrast, the delayed enzymatic peaks in orange indicate a more controlled, gradual oxidative response, consistent with the lower metabolic rate of non-climacteric fruits.

As ripening progresses, particularly in climacteric fruits such as papaya, the balance between ROS production and antioxidant defenses becomes critical. Increased respiratory activity enhances ROS generation, and insufficient detoxification can lead to membrane damage, enzyme degradation, and tissue softening (Kan et al., 2025). Therefore, UV-C-induced activation of antioxidant enzymes, such as catalase and peroxidase, may help delay senescence by maintaining cellular integrity and limiting oxidative damage.

Evidence from the literature supports this mechanism, as UV-C treatments have been shown to increase catalase and peroxidase activities in pears (Sun et al., 2022) and strawberries (Jin et al., 2017), thereby delaying ripening and improving postharvest quality. In the present study, the differences in activity between papaya and orange further highlight species-specific patterns of oxidative stress regulation. In papaya, consistently elevated activity indicates a greater capacity for ROS detoxification, whereas in orange, the later enzymatic peak suggests a more moderate and regulated adaptive response. These findings indicate that UV-C modulates antioxidant and defense systems through ROS-mediated signaling, with responses depending on the metabolic characteristics and stress tolerance of each species.

Although the experiments were conducted under controlled laboratory conditions, the UV-C doses applied in this study are within the range commonly reported for postharvest treatment systems (Tchonkouang et al., 2023). These doses can be achieved in commercial packinghouses; however, before industrial application, the system should be validated under real processing conditions, including larger treatment volumes.

In summary, UV-C radiation controls anthracnose and sour rot, likely through a combination of direct effects and/or host defense response induction. Moreover, it delayed ripening- and senescence-related processes, preserving firmness, color, acidity, epidermal integrity, and reducing weight loss.

Thus, modulation of UV-C radiation emerges as a promising and sustainable strategy for postharvest disease control, reducing the risk of thermal injury while maintaining applicability to both UV-C-sensitive climacteric fruits, such as papaya, and more tolerant non-climacteric fruits, such as orange.

5. Conclusion

UV-C radiation modulation proved to be an effective strategy for controlling postharvest fungal diseases in papaya and orange, enabling optimized energy delivery with reduced thermal damage while preserving tissue integrity.

In papaya fruit, the modulated frequency (30 Hz/20 s / 0.44 kJ m^{-2}) provided the most favorable results, preserving epidermal integrity while reducing anthracnose development. In orange fruit, continuous application (0 Hz/30 s / 1.99 kJ m^{-2}) produced similar reductions in disease without visible peel injury, demonstrating greater thermal tolerance. These species-dependent responses demonstrate that treatment effectiveness is influenced by the physiological characteristics and thermal sensitivity of each fruit.

UV-C exposure was associated with increased activity of antioxidant and defense-related enzymes, suggesting the induction of protective mechanisms that likely contributed to delayed ripening and senescence. These biochemical responses, combined with possible direct impacts on the pathogen, were accompanied by improved maintenance of firmness, acidity, and color, confirming preservation of physicochemical quality.

Overall, modulated UV-C application represents a promising non-chemical strategy for postharvest disease control in both climacteric and non-climacteric fruits, minimizing thermal injury, extending shelf life, and demonstrating strong potential for commercial application.

CRediT authorship contribution statement

Elke Simoni Dias Vilela: Writing – review & editing, Methodology. **Bernardo de Almeida Halfeld-Vieira:** Writing – review & editing, Methodology. **Juliana Aparecida Fracarolli:** Writing – review & editing, Supervision. **da silva Adriane Maria:** Writing – review & editing, Writing – original draft, Validation, Methodology, Investigation, Formal analysis. **Daniel Terao:** Writing – review & editing, Supervision, Project administration, Methodology, Funding acquisition. **Aline de Holanda Nunes Maia:** Writing – review & editing, Formal analysis. **Itala Suzana Oliveira Silva:** Writing – review & editing, Investigation. **Katia de Lima Nechet:** Writing – review & editing, Methodology. **Washington Luiz de Barros Melo:** Writing – review & editing, Methodology, Investigation.

Funding

This work was supported by the Fundação de Amparo à Pesquisa do Estado de São Paulo - FAPESP 2018/25318–7, the National Council for Scientific and Technological Development - CNPq 407421/2021–1, and a doctoral fellowship from CNPq (grant no. 140679/2022–7).

The Article Processing Charge (APC) for this publication was funded by the Coordination for the Improvement of Higher Education Personnel – CAPES (ROR identifier: 00x0ma614). For the purposes of open access, the authors have applied a Creative Commons CC BY license to any accepted version of the manuscript.

Declaration of Competing Interest

The authors declare that they have no known competing financial interests or personal relationships that could have appeared to influence the work reported in this paper.

Acknowledgements

The authors acknowledge the National Council for Scientific and Technological Development (CNPq; Project No. 140679/2022–7) for the doctoral scholarship awarded to Adriane Maria da Silva. The authors thank Rosely dos Santos Nascimento (Embrapa Meio Ambiente) and Rosa Helena Aguiar, Adriana Naomi Owada Ono, and Leandro Morais (FEAGRI/UNICAMP) for their assistance with laboratory analyses. The authors also acknowledge Ricardo Bazzani and Alfacitrus – Produção e

Comércio de Citrus, particularly Marcella Buzo da Fonseca, for their support in developing this research. The acknowledgements provided adhere to the journal's ethical and editorial requirements. The authors acknowledge the Coordination for the Improvement of Higher Education Personnel (CAPES, ROR identifier: 00x0ma614) for financial support.

Appendix A. Supporting information

Supplementary data associated with this article can be found in the online version at doi:10.1016/j.postharvbio.2026.114388.

Data availability

Data will be made available on request.

References

Abdipour, M., Hosseinifarahi, M., Naseri, N., 2019. Combination method of UV-B and UV-C prevents post-harvest decay and improves organoleptic quality of peach fruit. Sci. Hortic. 256, 108564. https://doi.org/10.1016/j.scienta.2019.108564.

Abdipour, M., Sadat Malekhossini, P., Hosseinifarahi, M., Radi, M., 2020. Integration of UV irradiation and chitosan coating: A powerful treatment for maintaining the postharvest quality of sweet cherry fruit. Sci. Hortic. 264, 109197. https://doi.org/10.1016/j.scienta.2020.109197.

Acevedo-Daza, J., Villegas Ciro, J.A., Pineda Sepulveda, V., Jaramillo González, J.C., Restrepo Cubillos, V., Peña García, J.T., Soto Bastidas, J.H., Buitrago Pinilla, L.T., Arroyo Merino, J.V., Ñañez Palacio, D.C., Castro Vargas, D.F., Largo Ávila, E., Garzón García, A.M., 2024. Effect of UV-C on postharvest quality of citrus fruits from the northeastern region of Valle del Cauca, Colombia. Biotecnia 26, 379–386. https://doi.org/10.18633/biotecnia.v26.2303.

Aebi, H., 1984. Catalase *in vitro*. in: Methods in Enzymology. Elsevier, pp. 121–126. https://doi.org/10.1016/S0076-6879(84)05016-3.

Consultas, AleloMicro, 2025. Empresa Bras. Pesqui. Agropecuária Embrapa. URL https://am.cenargen.embrapa.br/amconsulta/colecao?id=4 / (accessed 8 May 2026).

Armagan, H.S., Demirci, A., 2025. Current status of pulsed UV light technology for food, water, and food processing surface decontamination. Food Eng. Rev. 17, 966–993. https://doi.org/10.1007/s12393-025-09428-3.

Baligad, J.L., Huang, P.-L., Do, Y.-Y., 2023. The effects of UV-C irradiation and low temperature treatment on microbial growth and oxidative damage in fresh-cut bitter gourd (Momordica charantia L.). Horticulturae 9, 1068. https://doi.org/10.3390/horticulturae9101068.

Baracat-Pereira, M.C., De Almeida Oliveira, M.G., De Barros, E.G., Moreira, M.A., Santoro, M.M., 2001. Biochemical properties of soybean leaf lipoxygenases:Presence of soluble and membrane-bound forms. Plant Physiol. Biochem 39, 91–98. https://doi.org/10.1016/S0981-9428(00)01223-7.

Bolton, J.R., 2000. Calculation of ultraviolet fluence rate distributions in an annular reactor: significance of refraction and reflection. Water Res 34, 3315–3324. https://doi.org/10.1016/S0043-1354(00)00087-7.

Bornal, D.R., Silvestrini, M.M., Pio, L.A.S., Costa, A.C., Peche, P.M., Ramos, M.C.P., 2021. Brazilian position in the international fresh fruit trade network. Rev. Bras. Frutic. 43, e-021. https://doi.org/10.1590/0100-29452021021.

Bradford, M.M., 1976. A rapid and sensitive method for the quantitation of microgram quantities of protein utilizing the principle of protein-dye binding. Anal. Biochem 72, 248–254. https://doi.org/10.1016/0003-2697(76)90527-3.

Campbell, C.L., Madden, L.V., 1990. Introduction to Plant Disease Epidemiology, 1st Edition. ed.

Castillejo, N., Martínez-Zamora, L., Artés-Hernández, F., 2022. Postharvest UV radiation enhanced biosynthesis of flavonoids and carotenes in bell peppers. Postharvest Biol. Technol. 184, 111774. https://doi.org/10.1016/j.postharvbio.2021.111774.

Cháfer, M., Sánchez-González, L., González-Martínez, Ch, Chiralt, A., 2012. Fungal decay and shelf life of oranges coated with chitosan and bergamot, thyme, and tea tree essential oils. J. Food Sci. 77. https://doi.org/10.1111/j.1750-3841.2012.02827.x.

Chitarra, M.I.F., Chitarra, A.B., 2005. Postharvest of fruits and vegetables: physiology and handling. UFLA.

Cui, X., Bassey, A.P., Wang, F., Xie, S., Li, D., Fan, L., Zhu, Y., Bin, L., Liu, X., 2026. Inactivation of Penicillium ochrochloron spores by pulsed light: Mechanism and preservation efficacy in strawberries. Food Control 179, 111569. https://doi.org/10.1016/j.foodcont.2025.111569.

Da Silva, A.M., Terao, D., Terra, L.R., De Holanda Nunes Maia, A., Fracarolli, J.A., 2023. Control of sour rot in 'Lima' orange using hot water treatment and UV-C radiation. Trop. Plant Pathol. 48, 547–555. https://doi.org/10.1007/s40858-023-00595-4.

Deng, Y., Lu, S., 2017. Biosynthesis and Regulation of Phenylpropanoids in Plants. Crit. Rev. Plant Sci. 36, 257–290. https://doi.org/10.1080/07352689.2017.1402852.

Dixon, R.A., 2001. Natural products and plant disease resistance. Nature 411, 843–847. https://doi.org/10.1038/35081178.

Duque-Sarango, P., Delgado-Armijos, N., Romero-Martínez, L., Pinos-Vélez, V., 2023. Assessing the potential of ultraviolet irradiation for inactivating waterborne fungal spores: kinetics and photoreactivation studies. Front. Environ. Sci. 11, 1212807. https://doi.org/10.3389/fenvs.2023.1212807.

Erkan, M., Wang, S.Y., Wang, C.Y., 2008. Effect of UV treatment on antioxidant capacity, antioxidant enzyme activity and decay in strawberry fruit. Postharvest Biol. Technol. 48, 163–171. https://doi.org/10.1016/j.postharvbio.2007.09.028.

Esua, O.J., Chin, N.L., Yusof, Y.A., Sukor, R., 2020. A Review on Individual and Combination Technologies of UV-C Radiation and Ultrasound in Postharvest Handling of Fruits and Vegetables. Processes 8, 1433. https://doi.org/10.3390/pr8111433.

Fabi, J.P., Do Prado, S.B.R., 2019. Fast and Furious: Ethylene-Triggered Changes in the Metabolism of Papaya Fruit During Ripening. Front. Plant Sci. 10, 535. https://doi.org/10.3389/fpls.2019.00535.

Fisher, R.A., 1922. On the Interpretation of χ 2 from Contingency Tables, and the Calculation of P. J. R. Stat. Soc. 85, 87. https://doi.org/10.2307/2340521.

Gąstoł, M., Białaszczyk, U., 2024. Effect of Magnetic Field and UV-C Radiation on Postharvest Fruit Properties. Agriculture 14, 1167. https://doi.org/10.3390/agriculture14071167.

Hammerschmidt, R., Nuckles, E.M., Kuć, J., 1982. Association of enhanced peroxidase activity with induced systemic resistance of cucumber to Colletotrichum lagenarium. Physiol. Plant Pathol. 20, 73–82. https://doi.org/10.1016/0048-4059(82)90025-X.

Hu, L., Yang, C., Zhang, L., Feng, J., Xi, W., 2019. Effect of Light-Emitting Diodes and Ultraviolet Irradiation on the Soluble Sugar, Organic Acid, and Carotenoid Content of Postharvest Sweet Oranges (*Citrus sinensis* (L.) Osbeck). Molecules 24, 3440. https://doi.org/10.3390/molecules24193440.

Instituto Adolfo Lutz, 2008. Métodos físico-químicos para análise de alimentos. ⟨https://wp.ufpel.edu.br/nutricaobromatologia/files/2013/07/NormasADOLFOLUTZ.pdf⟩ / (accessed 03 March 2026).

Islam, T., Danishuddin, Tamanna, N.T., Matin, M.N., Barai, H.R., Haque, M.A., 2024. Resistance mechanisms of plant pathogenic fungi to fungicide, environmental impacts of fungicides, and sustainable solutions. Plants 13, 2737. https://doi.org/10.3390/plants13192737.

Jin, P., Wang, H., Zhang, Y., Huang, Y., Wang, L., Zheng, Y., 2017. UV-C enhances resistance against gray mold decay caused by Botrytis cinerea in strawberry fruit. Sci. Hortic. 225, 106–111. https://doi.org/10.1016/j.scienta.2017.06.062.

Kabir, Md.Y., Hossain, S.K., 2025. Botanical extracts improve postharvest quality and extend the shelf life of papaya (*Carica papaya* L. cv. Shahi). N. Z. J. Crop Hortic. Sci. 53, 605–621. https://doi.org/10.1080/01140671.2024.2348137.

Kan, J., Gao, M., Dong, W., Tang, C., Qian, C., Liu, J., 2025. Impact of Ultraviolet-C Light on Softening and Senescence During Storage of Peach Fruit. J. Food Biochem 2025, 5341034. https://doi.org/10.1155/jfbc/5341034.

Khamsaw, P., Sangta, J., Chaiwan, P., Rachtanapun, P., Sirilun, S., Sringarm, K., Thanakkasaranee, S., Sommano, S.R., 2022. Bio-Circular Perspective of Citrus Fruit Loss Caused by Pathogens: Occurrences, Active Ingredient Recovery and Applications. Horticulturae 8, 748. https://doi.org/10.3390/horticulturae8080748.

Konietschke, F., Placzek, M., Schaarschmidt, F., Hothorn, L.A., 2015. nparcomp: An Software Package for Nonparametric Multiple Comparisons and Simultaneous Confidence Intervals. J. Stat. Softw. 64. https://doi.org/10.18637/jss.v064.i09.

Kuck, L.S., Noreña, C.P.Z., 2021. Effect of UV-C Irradiation on Quality from Fresh Grapes var. Bordô. Braz. Arch. Biol. Technol. 64, e21200735. https://doi.org/10.1590/1678-4324-2021200735.

Levene, H., 1960. Robust Tests for Equality of Variances. In: Olkin, I., et al. (Eds.), Contributions to Probability and Statistics: Essays in Honor of Harold Hotelling, 2. Stanford University Press, Palo Alto, pp. 278–292.

Maldonado, A.F.S., Schieber, A., Gänzle, M.G., 2015. Plant defence mechanisms and enzymatic transformation products and their potential applications in food preservation: Advantages and limitations. Trends Food Sci. Technol. 46, 49–59. https://doi.org/10.1016/j.tifs.2015.07.013.

Mansur, A.R., Lee, H.S., Lee, C.J., 2023. A Review of the Efficacy of Ultraviolet C Irradiation for Decontamination of Pathogenic and Spoilage Microorganisms in Fruit Juices. J. Microbiol. Biotechnol. 33, 419–429. https://doi.org/10.4014/jmb.2212.12022.

Mayer, A.M., 2006. Polyphenol oxidases in plants and fungi: Going places? A review. Phytochemistry 67, 2318–2331. https://doi.org/10.1016/j.phytochem.2006.08.006.

Menaka, M., Asrey, R., Vinod, B.R., Ahamad, S., Meena, N.K., Bhan, C., Goswami, A.K., 2024. UV-C Irradiation Enhances the Quality and Shelf-Life of Stored Guava Fruit via Boosting the Antioxidant Systems and Defense Responses. Food Bioprocess Technol. 17, 3704–3715. https://doi.org/10.1007/s11947-024-03338-8.

Miranda, M., Sun, X., Marín, A., Dos Santos, L.C., Plotto, A., Bai, J., Benedito Garrido Assis, O., David Ferreira, M., Baldwin, E., 2022. Nano- and micro-sized carnauba wax emulsions-based coatings incorporated with ginger essential oil and hydroxypropyl methylcellulose on papaya: Preservation of quality and delay of postharvest fruit decay. Food Chem. X 13, 100249. https://doi.org/10.1016/j.fochx.2022.100249.

Mohamed, N.T., Ding, P., Kadir, J., M. Ghazali, H., 2017. Potential of UVC germicidal irradiation in suppressing crown rot disease, retaining postharvest quality and antioxidant capacity of *Musa* AAA "Berangan" during fruit ripening. Food Sci. Nutr. 5, 967–980. https://doi.org/10.1002/fsn3.482.

Pascholati, S.F., Nicholson, R.L., Butler, L.G., 1986. Phenylalanine Ammonia-Lyase Activity and Anthocyanin Accumulation in Wounded Maize Mesocotyls. J. Phytopathol. 115, 165–172. https://doi.org/10.1111/j.1439-0434.1986.tb00874.x.

Passardi, F., Penel, C., Dunand, C., 2004. Performing the paradoxical: how plant peroxidases modify the cell wall. Trends Plant Sci. 9, 534–540. https://doi.org/10.1016/j.tplants.2004.09.002.

Pathare, P.B., Opara, U.L., Al-Said, F.A.-J., 2013. Colour Measurement and Analysis in Fresh and Processed Foods: A Review. Food Bioprocess Technol. 6, 36–60. https://doi.org/10.1007/s11947-012-0867-9.

Phannakham, N., Saepaisan, S., Hongpakdee, P., Ayutthaya, S.I.N., Lin, H.-L., Nampila, S., 2026. Influences of UV-C radiation on quality, antioxidant and disease control in 'Nam Dok Mai Sithong' mangoes during low temperature storage. Sci. Hortic. 355, 114595. https://doi.org/10.1016/j.scienta.2025.114595.

Philips Lighting, 2022. UV-C disinfection lamps: Product catalog ⟨https://www.assets.signify.com/is/content/Signify/Assets/philips-lighting/global/20210322-philips-uvc-disinfection-lamps-catalog.pdf⟩ / (accessed 03 March 2026).

Phonyiam, O., Ohara, H., Kondo, S., Naradisorn, M., Setha, S., 2021. Postharvest UV-C Irradiation Influenced Cellular Structure, Jasmonic Acid Accumulation, and Resistance Against Green Mold Decay in Satsuma Mandarin Fruit (Citrus unshiu). Front. Sustain. Food Syst. 5, 684434. https://doi.org/10.3389/fsufs.2021.684434.

Pinto, L.K.D.A., Martins, M.L.L., Resende, E.D.D., Thièbaut, J.T.L., 2011. Atividade da pectina metilesterase e da β-galactosidase durante o amadurecimento do mamão cv. golden. Rev. Bras. Frutic. 33, 713–722. https://doi.org/10.1590/S0100-29452011005000087.

Pristijono, P., Bowyer, M.C., Papoutsis, K., Scarlett, C.J., Vuong, Q.V., Stathopoulos, C.E., Golding, J.B., 2019. Improving the storage quality of Tahitian limes (Citrus latifolia) by pre-storage UV-C irradiation. J. Food Sci. Technol. 56, 1438–1444. https://doi.org/10.1007/s13197-019-03623-x.

Pristijono, P., Bowyer, M.C., Scarlett, C.J., Vuong, Q.V., Stathopoulos, C.E., Golding, J.B., 2020. Postharvest UV-C treatment affects peel degreening 'Kensington Pride' mango fruit stored at 20°C. Acta Hortic. 215–220. https://doi.org/10.17660/ActaHortic.2020.1275.30.

Programa Brasileiro para Modernização da Horticultura, 2011. Normas de classificação de citros de mesa. ⟨https://ceagesp.gov.br/wp-ontent/uploads/2015/07/citros.pdf⟩ / (accessed 03 March 2026).

Programa Brasileiro para Modernização da Horticultura, 2003. Normas de classificação do mamão. ⟨https://minas1.ceasa.mg.gov.br/ceasainternet/_lib/file/docagroqcartilhas/MAMAO⟩(1).pdf / (accessed 03 March 2026).

Purwar, S., Gupta, S.M., Kumar, A., 2012. Enzymes of Phenylpropanoid Metabolism Involved in Strengthening the Structural Barrier for Providing Genotype and Stage Dependent Resistance to Karnal Bunt in Wheat. Am. J. Plant Sci. 03, 261–267. https://doi.org/10.4236/ajps.2012.32031.

R. Core Team, 2025. R: A Language and Environment for Statistical Computing_. R Foundation for Statistical Computing, Vienna, Austria. ⟨https://www.R-project.org⟩ / (accessed 03 March 2026).

Rabelo, M.C., Bang, W.Y., Nair, V., Alves, R.E., Jacobo-Velázquez, D.A., Sreedharan, S., De Miranda, M.R.A., Cisneros-Zevallos, L., 2020. UVC light modulates vitamin C and phenolic biosynthesis in acerola fruit: role of increased mitochondria activity and ROS production. Sci. Rep. 10, 21972. https://doi.org/10.1038/s41598-020-78948-1.

Rajapakshe, P., Rathnasinghe, N., Guruge, K., Nilmini, R., Jayasinghe, R., Karunaratne, V., Wijesena, R., Priyadarshana, G., 2025. Strategies to minimize post-harvest waste of fruits and vegetables: Current solutions and future perspectives. J. Future Foods, S277256692500045X. https://doi.org/10.1016/j.jfutfo.2025.04.013.

Ribeiro, J.G., Serra, I.M.R.S., Araújo, M.U.P., 2016. Uso de produtos naturais no controle de antracnose causado por *Colletotrichum gloeosporioides* em mamão. Summa Phytopathol. 42, 160–164. https://doi.org/10.1590/0100-5405/2023.

Ruiz, V.E., Interdonato, R., Cerioni, L., Albornoz, P., Ramallo, J., Prado, F.E., Hilal, M., Rapisarda, V.A., 2016. Short-term UV-B exposure induces metabolic and anatomical changes in peel of harvested lemons contributing in fruit protection against green mold. J. Photochem. Photobiol. B 159, 59–65. https://doi.org/10.1016/j.jphotobiol.2016.03.016.

Rutigliano, C.A.C., Di Pietro, C., Randis, F.N., Iacono, G., Toscano, G., Castello, I., Spartà, S., La Bella, E., Muratore, G., Vitale, A., 2025. Exploiting UV-C postharvest effects on brown rot management and shelf life of apricot fruit. J. Agric. Food Res. 24, 102458. https://doi.org/10.1016/j.jafr.2025.102458.

Santamera, A., Escott, C., Loira, I., Del Fresno, J.M., González, C., Morata, A., 2020. Pulsed Light: Challenges of a Non-Thermal Sanitation Technology in the Winemaking Industry. Beverages 6, 45. https://doi.org/10.3390/beverages6030045.

Sasaki, F.F.C., Ferracini, V.L., Queiroz, S.C.N., Tavares, M.M., Pereira, M.E.C., 2024. Multiresidue pesticide analysis to determine the influence of postharvest packinghouse handling on papaya residue levels. Pesqui. Agropecu. ária Bras. 59, e03506. https://doi.org/10.1590/s1678-3921.pab2024.v59.03506.

SAS/STAT, 2017. User's Guide: The GLM Procedure. ⟨https://documentation.sas.com/doc/en/statug/latest/statug_glm_overview.htm⟩ / (accessed 03 March 2026).

SAS/STAT, 2016. The MIXED Procedure. ⟨https://documentation.sas.com/doc/en/statug/latest/statug_mixed_overview.htm⟩ / (accessed 03 March 2026).

Scolfaro, F.P., Benato, E.A., Melo, W.L. de B., Sigrist, J.M.M., Vitali, A.A., Cia, P., Castro, M.F.P.M., 2007. Uso da Luz Branca Intensa Modulada para Controle de Doenças em Frutos Pós-colheita. Comun. Téc. Embrapa. ⟨https://www.infoteca.cnptia.embrapa.br/bitstream/doc/30789/1/CT872007.pdf⟩ / (accessed 03 March 2026).

Seshadri, N.M., Palanisamy, A.S., Mohanavelu, T., McDermott, O., 2024. Minimization of losses in postharvest of fresh produce supply chain. J. Agribus. Dev. Emerg. Econ. https://doi.org/10.1108/JADEE-04-2024-0139.

Söbeli, C., Uyarcan, M., Kayaardı, S., 2021. Pulsed UV-C radiation of beef loin steaks: Effects on microbial inactivation, quality attributes and volatile compounds. Innov. Food Sci. Emerg. Technol. 67, 102558. https://doi.org/10.1016/j.ifset.2020.102558.

Sripong, K., Jitareerat, P., Tsuyumu, S., Uthairatanakij, A., Srilaong, V., Wongs-Aree, C., Ma, G., Zhang, L., Kato, M., 2015. Combined treatment with hot water and UV-C elicits disease resistance against anthracnose and improves the quality of harvested mangoes. Crop Prot. 77, 1–8. https://doi.org/10.1016/j.cropro.2015.07.004.

Student, 1908. The Probable Error of a Mean. Biometrika 6 (1). https://doi.org/10.2307/2331554.

Sun, T., Ouyang, H., Sun, P., Zhang, W., Wang, Y., Cheng, S., Chen, G., 2022. Postharvest UV-C irradiation inhibits blackhead disease by inducing disease resistance and reducing mycotoxin production in 'Korla' fragrant pear (*Pyrus sinkiangensis*). Int. J. Food Microbiol 362, 109485. https://doi.org/10.1016/j.ijfoodmicro.2021.109485.

Tchonkouang, R.D., Lima, A.R., Quintino, A.C., Cristofoli, N.L., Vieira, M.C., 2023. UV-C Light: A Promising Preservation Technology for Vegetable-Based Nonsolid Food Products. Foods 12, 3227. https://doi.org/10.3390/foods12173227.

Terao, D., De Lima Nechet, K., Ponte, M.S., De Holanda Nunes Maia, A., De Almeida Anjos, V.D., De Almeida Halfeld-Vieira, B., 2017. Physical postharvest treatments combined with antagonistic yeast on the control of orange green mold. Sci. Hortic. 224, 317–323. https://doi.org/10.1016/j.scienta.2017.06.038.

Terao, D., Nechet, K.L., Frighetto, R.T.S., Anjos, V.D.A., Maia, A.H.N., Halfeld-Vieira, B. A., 2021. Control of Fusarium rot in Galia melon and preservation of fruit quality with UV-C radiation and hot water treatments. Trop. Plant Pathol. 46, 350–359. https://doi.org/10.1007/s40858-021-00432-6.

Ullah, I., Toor, M.D., Yerlikaya, B.A., Mohamed, HebaI., Yerlikaya, S., Basit, A., Rehman, A.U., 2024. High-temperature stress in strawberry: understanding physiological, biochemical and molecular responses. Planta 260, 118. https://doi.org/10.1007/s00425-024-04544-6.

Yamaga, I., Hamasaki, S., 2020. Seasonal Effect of Ultraviolet Irradiation on Polymethoxyflavone and Hesperidin Content in Ponkan and Tachibana Flavedo. HortScience 55, 1078–1082. https://doi.org/10.21273/HORTSCI15000-20.

Wang, F., Cao, C., Cai, Y., Chen, X., Lin, H., Cai, C., Zhu, R., 2025. Pulsed light treatment reduces the growth and patulin production of Penicillium expansum and its application in apple preservation. Food Control 177, 111433. https://doi.org/10.1016/j.foodcont.2025.111433.

Zou, H., Xiao, Q., Li, G., Wei, X., Tian, X., Zhu, L., Ma, F., Li, M., 2025. Revisiting the advancements in plant polyphenol oxidases research. Sci. Hortic. 341, 113960. https://doi.org/10.1016/j.scienta.2025.113960.